

Surface and tropospheric ozone over East Asia and Southeast Asia from observations: distributions, trends, and variability

Ke Li^{1,*,#}, Rong Tan^{1,#}, Wenhao Qiao^{1,#}, Taegyung Lee², Yufen Wang¹, Danyuting Zhang¹, Minglong Tang¹, Wenqing Zhao¹, Yixuan Gu¹, Shaojia Fan³, Jinqiang Zhang⁴, Xiaopu Lyu⁵, Likun Xue⁶, Jianming Xu^{7,8}, Zhiqiang Ma^{9,10}, Mohd Talib Latif¹¹, Teerachai Amnuaylojaroen¹², Junsu Gil¹³, Mee-Hye Lee¹³, Juseon Bak¹⁴, Joowan Kim¹⁵, Hong Liao¹, Yugo Kanaya¹⁶, Xiao Lu³, Tatsuya Nagashima¹⁷, Ja-Ho Koo^{2,*}

¹State Key Laboratory of Climate System Prediction and Risk Management, Joint International Research Laboratory of Climate and Environment Change, Jiangsu Key Laboratory of Atmospheric Environment Monitoring and Pollution Control, Collaborative Innovation Center of Atmospheric Environment and Equipment Technology, School of Environmental Science and Engineering, Nanjing University of Information Science and Technology, Nanjing 210044, China

²Department of Atmospheric Sciences, Yonsei University, Seoul 03722, South Korea

³School of Atmospheric Sciences, Sun Yat-sen University, Zhuhai, Guangdong, China

⁴State Key Laboratory of Atmospheric Environment and Extreme Meteorology, Institute of Atmospheric Physics, Chinese Academy of Sciences, Beijing 100029, China

⁵Department of Geography, Faculty of Social Sciences, Hong Kong Baptist University, Hong Kong, China

⁶Environment Research Institute, Shandong University, Qingdao, China

⁷Shanghai Typhoon Institute, Shanghai Meteorological Service, Shanghai 200030, China

⁸Shanghai Key Laboratory of Meteorology and Health, Shanghai Meteorological Service, Shanghai 200030, China

⁹Institute of Urban Meteorology, China Meteorological Administration, Beijing 100089, China

¹⁰Beijing Shangdianzi Regional Atmosphere Watch Station, Beijing 101507, China

¹¹Department of Earth Sciences and Environment, Faculty of Science and Technology, Universiti Kebangsaan Malaysia, Bangi, Selangor, Malaysia

¹²Atmospheric Pollution and Climate Change Research Units, School of Energy and Environment, University of Phayao, Phayao 56000, Thailand

¹³Department of Earth and Environment Sciences, Korea University, Seoul 02841, South Korea

¹⁴Institute of Environmental Studies, Pusan National University, Busan 46241, Republic of Korea

¹⁵Department of Atmospheric Sciences, Kongju National University, Kongju 32588, South Korea

¹⁶Japan Agency for Marine-Earth Science and Technology, Yokohama, Japan

¹⁷National Institute for Environmental Studies, Tsukuba 305-8506, Japan

[#]These authors contributed equally

**Correspondence to:* Ke Li (keli@nuist.edu.cn) and Ja-Ho Koo (zach45@yonsei.ac.kr)

Abstract. High level of ozone throughout the troposphere is an emerging concern over East Asia and Southeast Asia. Here we analyzed available surface ozone measurements in the past two decades (2005–2021) over eight countries, and ten ozonesonde and aircraft measurements within this region. At surface, seasonal mean ozone over 2017–2021 varies from 30 nmol mol⁻¹ (i.e., 30 ppb) in Southeast Asia to 75 nmol mol⁻¹ in summer in North China. The metric of seasonal 95th percentile ozone can identify the multiple hotspots of ozone pollution of over 85 nmol mol⁻¹ in Southeast Asia. The new WHO peak season ozone standard indicates that both East Asia and Southeast Asia face a widespread risk of long-term exposure. The surface ozone increase in South Korea and Southeast Asia from 2005 was leveling off or even decreased in the past decade, while ozone increase in 2000s over China has amplified after 2013. Surface ozone trends in Japan and Mongolia were flat in the past decade. In the troposphere, the available measurements show an overall increasing tendency at different altitudes from a three-decade perspective and its trend in the past decade remains unclear due to data availability. The difference in tropospheric ozone level between East Asia and Southeast Asia is likely due to the high background ozone from stratospheric intrusion over Northeast Asia. In terms of ozone controls, our results suggest that anthropogenic emissions determine the occurrence of high ozone levels but the underappreciated strong ozone climate penalty, particularly over Southeast Asia, will make ozone controls harder under a warmer climate.

1. Introduction

Tropospheric ozone has been a long-lasting threat to public health, crop yield, and climate warming (Chang et al., 2017; DeLang et al., 2021; Lyu et al., 2023). Its importance in dampening carbon sink of forests by reducing productivity is also increasingly recognized in recent years (Cheesman et al., 2024; Zhou et al., 2024). Tropospheric ozone is mainly produced from the photochemical reactions between nitrogen oxides (NO_x) and volatile organic compounds (VOCs) in the presence of sunlight; stratosphere-troposphere exchange (STE) can also transport ozone into the troposphere (Neu et al., 2014) and even reach up to the surface under conducive weather conditions (Chen et al. 2024). In particular, high level of tropospheric ozone over East Asia and Southeast Asia is of great concern. For example, the estimated cardiovascular premature mortality attributable to surface ozone is 277,800 (142,900–421,900) in 2019 over East Asia and Southeast Asia, accounting for ~50% of its global health burden (Sun et al., 2024). The current ozone exposure can reduce the annual crop yield in China, South Korea, and Japan, by ~60, 60, 20 million tonnes for wheat, rice, and maize, respectively (Feng et al.,

2022). As such, it is important to elucidate the spatiotemporal distributions of observed ozone from the surface to troposphere over East Asia and Southeast Asia.

Surface ozone concentrations have been measured by nation-level networks for more than one decade in many countries. In Japan, surface network since the 1970s revealed a gradual increase in ozone (Nagashima et al. 2017; Kawano et al., 2022) until the past decade where Japanese sites experienced an ozone decrease by $-0.8 \pm 0.5 \text{ nmol mol}^{-1} \text{ yr}^{-1}$ (Wang et al., 2024). In South Korea, surface ozone has been increasing in the past two decades, leading to the maximum daily 8 h average (MDA8) ozone often exceeding 80 nmol mol^{-1} in summer in the Seoul metropolitan area (Kim et al., 2023; Colombi et al., 2023). In China, national surface network was established in 2013 and the widespread rising surface ozone in the past decade positioned China to be one of countries with the highest ozone level worldwide (Lu et al., 2020; Li et al., 2021; Wang et al., 2024). In contrast, Hong Kong, located in China's southern coast, exhibited an overall increase in the surface ozone level by $0.35 \text{ nmol mol}^{-1} \text{ yr}^{-1}$ over 1994–2018, but the trend tended to level off in recent years (Wang et al., 2019).

In Southeast Asia, surface ozone levels are much smaller than those in East Asia due to the lower anthropogenic emissions and frequent marine air inflow (Ahamad et al., 2020; Sukkhum et al., 2022; Wang et al., 2022a). The previously published analyses on long-term ozone trends in Southeast Asia are scarce, mainly focused on Malaysia and Thailand before 2016. In Malaysia, there was observed ozone increase of $0.09\text{--}0.21 \text{ nmol mol}^{-1} \text{ yr}^{-1}$ over the Peninsular Malaysia during 1997–2016 but the Borneo Malaysia recorded small or insignificant ozone trends (Ahamad et al., 2020; Wang et al., 2022a). In Thailand, the observed surface ozone experienced significant increase by 0.7 to $1.2 \text{ nmol mol}^{-1} \text{ yr}^{-1}$ during dry seasons over 2005–2016 (Wang et al., 2022a). In Indonesia, there was no significant ozone trend in Bukit Koto Tabang (a suburban site) over 2005–2016 (Wang et al., 2022a). In Philippines, Salvador et al. (2022) reported an increase of $0.41 \text{ nmol mol}^{-1} \text{ yr}^{-1}$ in surface ozone over 2014–2020 based on air quality measurements in Butuan (an urban site), southern Philippines. Long-term ozone measurements in other Southeast Asia countries were not well documented.

Tropospheric ozone profiles and columns over East Asia and Southeast Asia have been measured by multiple platforms including ozonesonde, aircraft, and satellite. By using long-term ozonesonde measurements, previous studies have extensively explored tropospheric ozone profiles in Beijing (Zeng et al., 2023) and Hong Kong (Liao et al., 2020) of China, and in Pohang of South Korea (Bak et al., 2022). However, these ozonesonde-based analyses mainly focused on the spatiotemporal variability and source contributions of tropospheric ozone at the individual site. By using the IAGOS (In-Service Aircraft for a Global Observing System) aircraft ozone observations, Gaudel et al. (2020) show that tropospheric ozone level increases with latitude from Malaysia/Indonesia to Northeast

100 China/South Korea. More importantly, they reported a rapid tropospheric ozone increase in 1994–2016
101 over East Asia and Southeast Asia, consistent with satellite tropospheric ozone column trends
102 (Gopikrishnan and Kuttippurath, 2024), which has been further attributed to the rising anthropogenic
103 emissions both locally and remotely (Wang et al., 2022a; Wang et al., 2022b; Li et al., 2023).
104 Considering that East Asia and Southeast Asia has been identified as a global hot spot with the fastest
105 increase in observed tropospheric ozone after 1990s by the Intergovernmental Panel on Climate
106 Change (IPCC) Sixth Assessment Report (AR6), a comprehensive assessment on tropospheric ozone
107 over this region by using these available measurements is strongly needed.

108 Under the framework of the Tropospheric Ozone Assessment Report (TOAR, 2014–2019), the TOAR
109 documents comprehensively estimate the global ozone pollution and its historical trends. The first-
110 phase TOAR includes only limited ground observation data over East Asia and Southeast Asia
111 countries before 2014 (Chang et al., 2017). In the context of the TOAR Phase Two (TOAR II, 2020–
112 2024), the established East Asia Focus Working Group (EAWG) aims to advance ozone research over
113 East Asia and Southeast Asia, with a focus on observed ozone trends and their attributions. Our effort
114 is to include ozone measurements (or post-calculated ozone metrics) from surface to tropopause
115 collected from TOAR database and individual institutions over East Asia and Southeast Asia. Please
116 also see the accompanying paper for ozone trend attributions (Lu et al., 2024).

117 This paper will present the most comprehensive view of ozone distributions and evolution over East
118 Asia and Southeast Asia across different spatiotemporal scales in the past two decades. The structure
119 of this paper is as follows: Section 2 introduces the multiple ozone measurements and calculation of
120 different ozone metrics; Section 3 describes the present-day surface ozone levels with different metrics
121 and long-term surface ozone trends in the past two decades; Section 4 describes the three-dimensional
122 present-day distribution and long-term trends in tropospheric ozone; Section 5 discusses the important
123 implications for future ozone pollution controls; Conclusions are given in Section 6.

124

125 **2. Data and methods**

126 **2.1 Surface ozone observations**

127 The TOAR data portal archives a global comprehensive and freely accessible data collection of surface
128 ozone observations (<https://igacproject.org/activities/TOAR/TOAR-II>), which supports TOAR’s
129 assessment report of global ozone distributions and trends from surface to the tropopause. The TOAR
130 database keeps updated to include all recent observations since 2014. To give an up-to-date assessment
131 of tropospheric ozone over East Asia and Southeast Asia, here we take advantage of TOAR database

132 to examine ozone levels in different countries within the same time frame.

133 In this study, we used surface ozone measurements from national networks of China (2013–2021),
134 Japan (2005–2021), South Korea (2005–2021), Malaysia (2005–2021), and Thailand (2005–2021) that
135 were collected from the TOAR II database or provided by our EAWG members. In addition to the
136 national network records, individual ozone measurement in Ulaanbaatar of Mongolia, Phnom Penh of
137 Cambodia, and Bandung of Indonesia from the Acid Deposition Monitoring Network in East Asia
138 (EANET) was also included. To assess the long-term ozone trend in China before 2013, we also
139 collected 11 ozone measurements from previously-published literatures with updates from our EAWG
140 members. As shown in Table S1, it includes 1 global baseline station (Mt. Waliguan), 4 regional
141 background stations (Akedala, Longfengshan, Xianggelila, and Lin'an), and 1 rural station (Gucheng)
142 from Xu et al. (2020), 1 regional background station (Mt. Tai) from Sun et al. (2016), 1 regional
143 background station (Shangdianzi) from Ma et al. (2016), 1 urban station from Gu et al. (2020), and 1
144 urban station (Guangzhou) and 1 suburban station (Hong Kong) from Zhang et al. (2011).

145 To ensure data quality, the daily and monthly means were calculated using the hourly data when it has
146 over 75% valid data each day and month. To fully assess ozone distributions, we adopted the following
147 ozone metrics in this study: (1) Seasonal mean ozone. Seasonal MDA8 concentrations are calculated
148 for the four seasons (December-January-February, DJF; March-April-May, MAM; June-July-August,
149 JJA; September-October-November, SON), respectively. (2) Ozone exceedance. National ambient
150 ozone air quality standard varies greatly among countries in East Asia and Southeast Asia (Table S2).
151 The threshold for MDA8 ozone ranges from $60 \mu\text{g m}^{-3}$ in Philippines to $160 \mu\text{g m}^{-3}$ in China, and for
152 the maximum daily 1 h average (MDA1) ozone ranges from $120 \mu\text{g m}^{-3}$ in Japan to $235 \mu\text{g m}^{-3}$ in
153 Indonesia. Under standard conditions (1013 hPa, 273 K), $1 \text{ nmol mol}^{-1} = 2.14 \mu\text{g m}^{-3}$. In this study, we
154 adopted the thresholds of 60 nmol mol^{-1} and 47 nmol mol^{-1} (WHO standard) for MDA8 ozone to
155 determine the exceedance days. (3) Peak season ozone. In 2021, the World Health Organization (WHO)
156 newly introduced a standard for the peak season (six-month mean) ozone limit of $60 \mu\text{g m}^{-3}$ to save
157 more people suffering from its long-term exposure. We used this threshold to assessment the peak
158 season ozone levels.

159 **2.2 Tropospheric ozone observations**

160 In this part, we suggest our results from the analysis of vertical ozone profile, mostly based on the
161 ozonesonde measurement and some aircraft measurement. There are a number of ozonesonde
162 measurement sites, but here, we only consider 10 sites (Table S3), which has at least 10 measurement
163 years continuously for finding reliable trends by considering the lesson from Chang et al. (2024). If a

164 certain site is not satisfying with this standard, we only suggest the mean pattern of ozone vertical
165 profile for that site in order to show all existed data as possible as we can. This approach enables us to
166 compare with recent results produced from other ozonesonde data analyses (Gaudel et al., 2024;
167 Stauffer et al., 2024). Data at 9 sites were obtained from the World Ozone and Ultraviolet Radiation
168 Data Centre (WOUDC) and Southern Hemisphere ADditional OZonesondes (SHADOZ) data archive.
169 Data at Beijing site, which were utilized in the previous study (Zhang et al., 2021) were directly
170 provided from the measurement team.

171 We also used the altitudinal ozone measurements that have been collected from the In-service Aircraft
172 for a Global Observing System (IAGOS). While the IAGOS mission has been continued since 1990s
173 and still available, ozone data in East Asia are somewhat limited. Here we only utilized the IAGOS
174 ozone data from 1995 to 2022, the period having enough number of measurements, for the two defined
175 regions such as Northeast and Southeast Asia. Location of all ozonesonde sites and the IAGOS region
176 will be detailed in Section 4.1, and the number of all ozonesonde and IAGOS data used in this study
177 is shown in Figure S1.

178 **2.3 Ozone trend calculation**

179 Noticeable outliers are not detected in our dataset for both surface ozone and ozonesonde and IAGOS
180 datasets. In terms of ozone distributions, we present the present-day ozone maps averaged over 2017–
181 2021. We required that there are at least three out of these five years of data available in the calculation.
182 In terms of ozone trends: the time frame of 2013–2021 was adopted to represent the past decade trend;
183 the time frame of 2005–2021 was adopted to represent the 21st Century trend and time series should
184 begin at least in the range 2005–2010 and end in the range 2017–2021; the time frame of 1995–2021
185 was adopted to represent the late 20th century trend and time series should begin at least in the range
186 1995–1999 and end in the range 2017–2021.

187 Following TOAR II guideline, to determine the ozone trend, we first derived the monthly anomalies
188 of ozone concentrations that are calculated as the difference between the individual monthly means
189 and the monthly climatology. Then, a quantile regression method as recommended by TOAR II
190 statistical guidance was employed to estimate the linear trend in surface ozone, and a 50th quantile
191 regression slope was reported in consideration of the length of ozone records.

192

193

194

3. Present-day distribution and long-term trends in surface ozone

3.1 Distribution of present-day surface ozone over 2017–2021

3.1.1 Seasonal mean MDA8 ozone

Figure 1 shows the seasonal mean MDA8 ozone concentrations averaged over 2017–2021. In winter, seasonal mean ozone level is almost below 50 nmol mol⁻¹ due to the weak photochemistry. In many Chinese cities, ozone concentration is even decreased to 20–30 nmol mol⁻¹, and this is because the high NO_x emissions in urban environment (e.g., North China Plain) make ozone strongly titrated and often drop below the Northern Hemisphere background ozone (Vingarzan, 2004). High ozone values of 55–60 nmol mol⁻¹ in Northern Thailand and 60–65 nmol mol⁻¹ in Bangkok (Thailand) are notable. In spring, seasonal mean ozone concentrations are doubled in North China (north of 30°N) and increased by 10–20 nmol mol⁻¹ from wintertime in South Korea and Japan. High ozone of over 60 nmol mol⁻¹ in Thailand still holds in spring and ozone concentration is enhanced by up to 20 nmol mol⁻¹ in Yunnan province (China), reflecting a possible concentration from spring fire emissions over Southeast Asia (Xue et al., 2021). In summer, the highest ozone levels of over 75 nmol mol⁻¹ are found in the North China and western China exhibits ozone concentrations of 60–65 nmol mol⁻¹. In Southern China, ozone level is decreased to 30–55 nmol mol⁻¹ because of the active summer monsoon rainfall (Zhou et al., 2022). The hot spot of summer ozone pollution is found in Seoul (South Korea) where seasonal mean ozone is also over 75 nmol mol⁻¹, followed by 55–60 nmol mol⁻¹ in Tokyo (Japan), 40–50 nmol mol⁻¹ in Kuala Lumpur (Malaysia), 30–40 nmol mol⁻¹ in Bangkok (Thailand). In autumn, ozone concentrations are decreased strongly from their summer levels in the north of 30°N over East Asia but are increased remarkably in the Pearl River Delta (PRD) region of China where its seasonal mean MDA8 ozone of up to 65 nmol mol⁻¹ is the highest level within the East Asia and Southeast Asia.

In addition to mean ozone level, Figure 2 shows the seasonal 95th percentile ozone concentrations averaged over 2017–2021. The ozone metric is almost the fifth highest value in each season, representing the high ozone values of great concern in air quality management. Although the seasonality of the 95th percentile ozone resembles the mean ozone evolution, the occurrence of the very high 95th percentile ozone values highlights the severity of ozone pollution over East Asia and Southeast Asia. In winter, high ozone of 85–95 nmol mol⁻¹ occurs over the Southern Thailand, and some cities in PRD region can suffer from ozone level over 75 nmol mol⁻¹. In spring, in East Asia the 95th percentile ozone can reach over 95 nmol mol⁻¹ over Chinese major city clusters and Seoul, and in Southeast Asia ozone level of over 75 nmol mol⁻¹ occurs in many stations in Thailand and Peninsular Malaysia. In summer, high levels of the 95th percentile ozone appear exclusively over East Asia, with ozone concentrations of over 115 nmol mol⁻¹ in the North China Plain (NCP), over 105 nmol mol⁻¹ in

the Yangtze River Delta (YRD), and over 95 nmol mol⁻¹ in PRD, Sichuan Basin, Seoul, and Busan. In addition, some cities (e.g., Tokyo, Osaka) in Japan also have ozone levels over 85 nmol mol⁻¹. In autumn, the high ozone levels only concentrate on PRD and YRD regions, with the 95th percentile ozone over 115 nmol mol⁻¹ in PRD and over 95 nmol mol⁻¹ in YRD, respectively. However, Borneo Malaysia and Indonesia still record the 95th percentile ozone lower than 50 nmol mol⁻¹, suggesting the important role of fresh marine air inflow.

3.1.2 Number of days of ozone exceedance

Figure 3 shows that the national ozone air quality standard varies greatly in different countries over East Asia and Southeast Asia. For example, MDA8 and MDA1 ozone thresholds in China are 160 µg m⁻³ and 200 µg m⁻³, respectively, which lie at the high end of the adopted standards. A lower standard of MDA8 of 140 µg m⁻³ in Thailand and of 120 µg m⁻³ in Vietnam, South Korea, and Singapore are adopted, while Laos, Myanmar, and Philippine adopt a standard consistent with or lower than the WHO guidance. In terms of MDA1, most of the countries adopt a threshold around 200 µg m⁻³. As such, for the sake of health impact assessment, here we adopted the uniform threshold of 60 nmol mol⁻¹ and the WHO guideline to estimate the annual ozone exceedance.

Figure 4 shows the annual number of days with MDA8 ozone concentration greater than 60 nmol mol⁻¹ (NDGT60) and with MDA8 ozone concentration greater than 47 nmol mol⁻¹ (NDGT47), respectively. In terms of NDGT60, most of the NCP cities in China have ozone exceedance over 125 days, followed by around 100 days in YRD, PRD, and Northwest China. In South Korea, most of the stations experience 60-100 days per year with daily MDA8 ozone over 60 nmol mol⁻¹, while in Japan it is almost less than 45 days except for a few cities. In Southeast Asia, NDGT60 is almost less than 75 days, and particularly Malaysia, Cambodia, and Indonesia have NDGT60 less than 15 days that is consistent with the very low 95th percentile ozone (Figure 2). If the WHO standard is applied, most of the cities in eastern China will have more than 150 days with MDA8 ozone exceedance, and this is also the case for western China. This suggests the pressing challenge to mitigate ozone pollution due to the large-scale high emissions in China. In South Korea, the NDGT47 is over 100 days for most of the stations, which is consistent with the high background ozone issue as reported by Columbi et al. (2023). Ozone exceedance over 100 days for NDGT47 can be also found in major cities in Japan, Thailand, and Malaysia.

3.1.3 Peak season ozone levels

In this study, we apply the new WHO standard for peak season ozone that was introduced in September 2021 to assess risks of long-term ozone exposure over East Asia and Southeast Asia, which has not

260 been examined in previous studies. Figure 5 shows the estimated peak season ozone concentration
 261 averaged over 2017-2021 and its ratio relative to the WHO standard. In China, the NCP region holds
 262 the highest peak season ozone of over 70 nmol mol⁻¹ that is about 2.5 times the WHO threshold,
 263 followed by 65 nmol mol⁻¹ in YRD, 55 nmol mol⁻¹ in PRD, SCB, and some cities of Northwest China.
 264 More importantly, the lowest peak season ozone in China is still higher than the WHO standard,
 265 suggesting the difficulty in mitigation long-term ozone exposure over China. In South Korea, the peak
 266 season ozone is well above 55 nmol mol⁻¹ and even higher than 60 nmol mol⁻¹, again reflecting the
 267 important role of background ozone in South Korea. In Japan, the peak season is mainly within the
 268 range from 40 to 55 nmol mol⁻¹, amounting to 1.5-2 times the WHO standard. In Ulaanbaatar of
 269 Mongolia, the peak season ozone is below 20 nmol mol⁻¹. In Southeast Asia, Thailand has the highest
 270 peak season ozone of over 60 nmol mol⁻¹ around Bangkok, and high values of 55-60 nmol mol⁻¹ are
 271 also found in the northern Thailand and southern coastal Thailand. In Malaysia, the Peninsular
 272 Malaysia has peak season ozone of 30-50 nmol mol⁻¹, higher than the WHO standard. However, similar
 273 with the low seasonal mean values, the Borneo Malaysia, Cambodia, and Indonesia record peak season
 274 ozone lower than the WHO standard. Overall, the estimated peak season ozone level shows that 98%
 275 stations in East Asia and Southeast Asia are above the WHO standard, and suggests the urgent need to
 276 reduce long-term ozone exposure risks.

277 **3.1.4 Ozone climate penalty**

278 In addition to surface ozone distributions, the metric of ozone climate penalty is also very important
 279 for understanding ozone levels under a warming change. Figure 6 shows the observed 50th percentile
 280 regression slope between MDA8 ozone and temperature in different seasons averaged over 2017-2021.
 281 In East Asia, the locations of high ozone-temperature slope of 3-5 nmol mol⁻¹ °C⁻¹ in different seasons
 282 are consistent with the observed high level of surface ozone. The highest slope of over 5-8 nmol mol⁻¹
 283 °C⁻¹ is found over the PRD and Sichuan Basin in summer. In contrast, low ozone-temperature slope
 284 of less than 1 nmol mol⁻¹ °C⁻¹ across different seasons can be also found in some sites over Japan and
 285 Tibetan Plateau of China, suggesting a minimal role of local ozone photochemical formation in these
 286 remote sites. In Southeast Asia, however, we find a widespread high ozone-temperature slope. In
 287 Thailand, the ozone-temperature slope of over 3 nmol mol⁻¹ °C⁻¹ can be found throughout the year
 288 except for summer. In Malaysia, a strong slope of 4-8 nmol mol⁻¹ °C⁻¹ persists all the year around that
 289 is consistent with a ten-year analysis in Kuala Lumpur by Ashfold et al. (2024). More importantly, the
 290 observed 95th percentile regression shows a notably increased ozone-temperature slope over Southeast
 291 Asia (Figure S2), suggesting a stronger ozone climate penalty under extreme conditions. In contrast,
 292 the IPCC AR6 only identified East Asia and India as the hotspot of ozone climate penalty (Zanis et al.,

293 2022). Our observed-based results highlight the strongly underestimated ozone climate penalty over
294 Southeast Asia.

295 Considering the meteorological features may be quite different in different latitudes, we conducted
296 additional analysis on the relationship between ozone and other meteorological features (Figure S3-
297 S7). The widespread positive (negative) correlation between ozone and temperature (relative humidity),
298 reflecting the known conducive condition for ozone photochemistry. However, the synoptic patterns
299 that are important for ozone transport varied greatly at a regional scale. For example, in Figure S6,
300 summertime southerly winds are conducive for ozone pollution over North China by transporting
301 ozone precursors and warmer air, but would decrease ozone over Southern China by carrying with
302 cleaner marine inflow. As such, identifying the key synoptic pattern will be also necessary for
303 understanding local ozone variations under climate change. It also deserves further study of cluster
304 analysis about the ozone origin by transport or by precursors by taking advantage of this considerable
305 ozone data records.

306

307 **3.2 Surface ozone trends in the past two decades**

308 **3.2.1 2005-2021 ozone trends**

309 Figure 7 shows the observed ozone trends in different seasons over the period of 2005-2021. Due to
310 the availability of long-term surface measurements, we only present ozone trends over South Korea,
311 Japan, Thailand, and Malaysia. In South Korea, increasing ozone trends with high certainty are notable
312 across different seasons ranging from $0.48 \text{ nmol mol}^{-1} \text{ yr}^{-1}$ in winter to $0.96 \text{ nmol mol}^{-1} \text{ yr}^{-1}$ in summer.
313 In Japan, observed ozone shows a decreasing tendency from 2005 to 2021 in summer but an extensive
314 ozone increase by $0.28 \text{ nmol mol}^{-1} \text{ yr}^{-1}$ in wintertime. In Thailand, there is an overall increasing trend
315 in surface ozone but with spatial heterogeneity over 2005-2021. Specifically, significant ozone
316 increase mainly occurs over northern Thailand and southern coastal Thailand, while ozone increase
317 around Bangkok is much smaller or insignificant. In Malaysia, there is a wintertime ozone increase by
318 $0.2 \text{ nmol mol}^{-1} \text{ yr}^{-1}$ particularly in three sites in Peninsular Malaysia and in five sites in Borneo
319 Malaysia, while in other seasons the observed ozone trends over 2005-2021 are small and statistically
320 insignificant. The estimated increasing tendency in surface ozone since 2005 is in agreement with Kim
321 et al (2023) for 2001-2021 ozone increase in South Korea and with Wang et al. (2022) for 2005-2016
322 ozone increase in Southeast Asia.

323 Due to the lack of national network measurement before 2013 in China, we also complied 11 individual
324 ozone measurements (8 background/rural sites and 3 urban sites) that are available from around 2005

(see Data and methods). Figure 8 and Table S1 show the estimated seasonal ozone trends in these 11 stations by using the metrics of MDA8 ozone and 24-hour mean ozone. The Mt. Waliguan, a global baseline station of the World Meteorological Organization /Global Atmosphere Watch (Xu et al., 2020), shows statistically significant ozone increase by $0.56 \text{ nmol mol}^{-1} \text{ yr}^{-1}$ in spring. However, at the multiple regional background stations located in western boundary of China (Xianggelila, Akedala) and eastern boundary of China (Lin'an, Longfengshan), there is no such a consistent ozone increase but with large variability across different seasons, suggesting the important role of regional emission change and climate variability (Zhang et al. 2023, Ye et al., 2024). In the NCP, one of the regions with the highest present-day ozone level, the observed ozone after 2005 at the regional background sites (Shangdianzi, Mt. Tai) and rural site (Gucheng) experienced a consistently increasing trend in spring and summer seasons. In Shangdianzi, the MDA8 ozone trend over 2005-2019 is $0.85 \text{ nmol mol}^{-1} \text{ yr}^{-1}$ ($p < 0.1$) in spring and $0.73 \text{ nmol mol}^{-1} \text{ yr}^{-1}$ ($p = 0.12$) in summer, respectively. The similar seasonal trends are also shown in Gucheng (a rural site close to Shangdianzi) and Mt. Tai (located in the center of NCP). It is noted that summer ozone trends in Mt. Tai over 2005-2019 also have strong intraseasonal variability, with much faster ozone increase in July and August (Sun et al., 2016). In addition to the background/rural sites, urban sites in YRD (Xujiahui) and PRD (Guangzhou, Hong Kong) record the urban ozone increase after 2005 that has been attributed to anthropogenic emissions and circulation patterns in previous studies (Wang et al., 2019; Gu et al., 2020; Cao et al., 2024).

3.2.2 2013-2021 ozone trends

Figure 9 shows the observed ozone trends in different seasons over the period of 2013-2021. Here we include ozone trends over China, Mongolia, Japan, South Korea, Malaysia, and Thailand. In China, there is a widespread ozone increase throughout the year, with mean ozone increase of $1.0\text{-}1.2 \text{ nmol mol}^{-1} \text{ yr}^{-1}$ in different seasons, which is only half of the ozone increase over 2013-2019 in China (Lu et al., 2020; Li et al., 2020). Spatially, ozone increase mainly occurs in the northern China and western China. Seasonally, there is fast ozone increase in winter over the NCP region, suggesting the urgency of wintertime ozone regulation (Li et al., 2021). In South Korea, the 2005-2021 ozone rise is strongly mitigated over 2013-2021 when summer ozone trend is only $0.45 \text{ nmol mol}^{-1} \text{ yr}^{-1}$. In Mongolia, there is a notable spring ozone increase but with low certainty. In Southeast Asia, however, the observed ozone in Malaysia and Thailand shows a decreasing tendency in most of the sites, which is contrary to the overall ozone increase from 2005 to 2021. Overall, except for the rapid ozone increase over China in the past decade, there is a leveling off or decrease in surface ozone trend over other countries in the meantime.

To further examine the long-term ozone variability, we also show the time series of observed national

MDA8 ozone concentrations during warm seasons from 2005 to 2021 in Figure 10. In South Korea, there is a flat trend in ozone over 2017-2021 after a sustained ozone increase since 2005, and there is no clear trend in warm-season ozone in Japan due to the limited data availability. In Southeast Asia, after 2013, surface ozone in Malaysia starts to decline and ozone trend in Thailand levels off. This is also demonstrated in the warm-season ozone trend in Figure S8. In addition, we also find the large interannual variability in observed ozone concentration that deserves further investigation. For example, in 2017, there is strong surface ozone enhancement relative to 2016 in China, Japan, and South Korea, while surface ozone is consistently decreased in Mongolia, Thailand, and Malaysia. Previous studies have linked the changes in large-scale circulations to this extensive ozone anomalies (e.g., Yin et al., 2010; Jiang et al., 2021).

368

4. Present-day distribution and long-term trends in tropospheric ozone profiles

4.1 Three-dimensional distribution of present-day tropospheric ozone

First, we compared climatological mean vertical ozone profile (from surface to 10 km altitude) using the ozonesonde data (Figure 11). Beijing site in China shows the highest, but Kuala Lumpur site in Malaysia shows the lowest ozone mean values through the troposphere. In general, ozone values in East Asia (Beijing in China, Pohang in Korea, and Tsukuba in Japan) are higher than those in Southeast Asia (Kuala Lumpur in Malaysia and Watukosek in Indonesia). This pattern is also found when we compared average ozone values at 1, 3, 5, and 7 km altitudes (Figure 12). While some sites show the higher ozone values in the boundary layer (e.g., Watukosek), but generally free tropospheric (above 1-2 km height) ozone values are higher. Especially, Beijing, Pohang, Sapporo, and Tsukuba sites show large enhancement of ozone above 8 km altitude (Figure 12a), implying that the stratospheric ozone is strongly intruding into the troposphere. Actually ozone values in these 4 sites are highest at 3, 5, and 7 km altitudes, indicating the effect of stratospheric ozone to the enhancement of upper tropospheric ozone. These 4 sites are located over Japan and the Korean peninsula (Figure 11) where sudden increase of ozone usually occurs below the tropopause (Park et al., 2012).

Seasonal pattern of vertical ozone profile was continually investigated (Figure 13). Tropospheric ozone values at Beijing, Pohang, Sapporo, and Tsukuba sites where strong stratospheric ozone intrusion occurs, are generally high in spring (MAM) and summer (JJA). This pattern can be explained by the frequent intrusion of stratospheric ozone in spring (Park et al., 2012), and strong photochemical ozone

388 production that is typical characteristic in summer. In several sites (e.g., Beijing and Tsukuba),
389 photochemical ozone production in summer makes the boundary layer ozone much higher than free-
390 tropospheric ozone. Stratospheric ozone intrusion in these 4 sites looks also strong in winter, but does
391 not result in high ozone in the boundary layer due to weak photochemistry in winter. Boundary layer
392 ozone values at Kagoshima (Japan), Naha (Japan), King's park (Hongkong), and Hanoi (Vietnam) that
393 are located below 30 °N, however, are lowest in summer. Considering that these sites are easily affected
394 by the inflow of maritime air mass under the trade-wind influence, this low summertime ozone can be
395 explained by the transport of humid and ozone-poor air mass from the ocean due to the monsoon
396 system (Zhao and Wang, 2018; Jiang et al., 2021). Sites in equatorial region (i.e., Kuala Lumpur and
397 Watukosek) do not have large seasonal difference of tropospheric ozone.

398 We repeated same analysis using the IAGOS data (Figure 14). IAGOS ozone profiles over Northeast
399 Asia also reveal the highest tropospheric ozone in summer (June), and lowest in winter (December).
400 We can also see large enhancement of summertime ozone in the boundary layer associated with strong
401 photochemistry, and high ozone in winter (DJF) and spring (MAM) above 8 km altitude, implying the
402 intrusion effect of stratospheric ozone. Monthly variation of ozone at multiple heights (Figure 13b)
403 illustrates a sharp drop of ozone from June to July, depicting the wash-out effect due to the rainy season
404 called Jangma (Korea) or Maiyu (China). Overall, ozone profile pattern in Northeast Asia from the
405 long-term aircraft monitoring is similar to findings based on ozonesonde measurements. Among them,
406 we would highlight that the site showing high tropospheric ozone (e.g., Beijing in China, Pohang in
407 Korea, Sapporo in Japan), which are located in Northeast Asia and latitude is higher than 35 °N (Table
408 S3), relate to the strong intrusion of stratospheric ozone. Considering recent studies addressing that
409 background ozone in Northeast Asia is unexpectedly high (Lee and Park, 2022; Columbi et al., 2023),
410 we need to put more weight on the study about the contribution of stratospheric air masses to the
411 Northeast Asian background ozone.

412 We also added analyzed results using the IAGOS measurements in Southeast Asia (Figure 14). It is
413 similar that ozone in spring (MAM) is the highest. However, ozone in winter (DJF) is not the lowest
414 but ozone in summer (JJA) is the lowest in Southeast Asia, probably due to the relatively stronger
415 precipitation in summer, and warmer temperature in winter, compared to the atmospheric condition in
416 Northeast Asia. Similar to the case in Northeast Asia mentioned above, some previous studies reported

417 cases of the tropospheric ozone enhancement in Southern China affected by the influence of typhoon
418 (Zhan and Xie, 2022; Li, F. et al., 2023), which are typically explained based on the stratospheric ozone
419 intrusion driven by the deep convection (Chen et al., 2022). While those reported cases look significant,
420 however, our results in sites typically affected by typhoon (e.g., Naha, King's park) reveal that it may
421 not contribute to significant increase of summertime mean tropospheric ozone.

422 As stated in chapter 2.2, there are additional ozonesonde sites in East Asia, but these sites do not have
423 long-term measurements. While we cannot provide the long-term trend values for these sites, at least
424 the seasonal mean pattern can be suggested in spite of their short history of measurements. In this
425 purpose, we added one more result showing the seasonal mean pattern of ozone vertical profile at
426 additional 6 sites not having ozonesonde measurements in continuous 10 years (Figure S9): 5 sites in
427 South Korea (Yongin, Osan, Seosan, Anmyeon, and Cheju) and 1 site in Taiwan (Taipei) obtained from
428 the experiment team (Kang et al., 2024) or from the WOUDC data archive. Owing to the short-term
429 property, we cannot generalize this result as the typical seasonal average. However, it seems that this
430 information will be a good reference when the vertical ozone distribution is needed in further studies
431 about the East Asian tropospheric ozone.

432 **4.2. Altitudinal long-term trends of tropospheric ozone**

433 In addition to the spatial distribution of tropospheric ozone, we investigated the long-term trend of
434 ozone values in a vertical scale using the ozonesonde measurements. We confirmed the time-series
435 analysis at each altitude (Figure S10) and performed the quantile regression. Finally, we estimated
436 long-term ozone trend in the troposphere (from surface to 10 km altitude) per 100 m interval vertically
437 with the certainty information (using median and p-value). These results are shown in Figure 15.

438 At first, we can see increasing trend of tropospheric ozone in most East Asian sites that we examined
439 based on the annual median value. Increasing trends of ozone values at Sapporo, Tsukuba, and Naha
440 look high certain through whole troposphere (Figures 15a, 15b, and 15e), and those at Pohang also
441 looks partially high certain. Ozone at Hanoi mostly shows increasing trends but having low certainty.
442 Ozone values in King's park, Kuala Lumpur, and Watukosek are only increasing in the boundary layer
443 (below ~2-3 km), but reveal almost no evident long-term trend in the free troposphere. Kagoshima and
444 Beijing sites are totally opposite: decreasing trends through whole troposphere. Ozone decrease at
445 Kagoshima mostly looks to have low certainty, but that at Beijing does not look clearly evident. In

446 brief, we can classify 3 types of long-term trends of tropospheric ozone in East Asia: (1) Increase
447 through whole troposphere, (2) Increase only in the boundary layer and no evident trend in the free
448 troposphere, and (3) Decrease through whole troposphere.

449 We also examined trends using the seasonal mean ozone values: spring (MAM) in Figure S11, summer
450 (JJA) in Figure S12, autumn (SON) in Figure S13, and winter (DJF) in Figure S14. Ozone increase at
451 Sapporo, Tsukuba and Naha, regions showing increasing trends of annual median ozone with high
452 certainty, is also high certain in summer, but less certain in other seasons. Ozone trends at Pohang are
453 seasonally different: increase in summer and autumn (Figures S12c and S13c), but decrease in the
454 wintertime upper troposphere (Figure S14c). Ozone trends at Hanoi are generally increasing in terms
455 of annual median value, but those almost become no evident in the seasonal analysis. Ozone values in
456 King's park, Kuala Kumpur, and Watukosek, similar to the annual median analysis, are increasing with
457 medium certainty in the boundary layer, particularly in spring and summer. In other seasons, however,
458 ozone trends at Hanoi become no evident.

459 Ozone trends at Kagoshima and Beijing are different from other sites, as shown in the annual median
460 analysis in Figure 15. They are also decreasing consistently in whole seasons. These decreasing trends
461 at Kagoshima and Beijing are not usually accompanied with high certainty, but decreasing trends at
462 Kagoshima in spring are high certain (Figure S11d). Although trend values are not largely evident,
463 tropospheric ozone decrease at Beijing is quite consistent in all seasons. Zhang et al. (2021) also treated
464 the variation of ozonesonde measurements at Beijing, and it looks that the stratospheric ozone intrusion
465 is strong from 2006 to 2012 but not in other years, which may be related to the ozone trend at Beijing.
466 At this present moment, these decreasing trends were not well explained by our knowledge.
467 Nonetheless, we would report these trends because it can be a motivation of further research.

468 We finally estimated the long-term trend of tropospheric ozone in East Asia using the IAGOS aircraft
469 measurements: Northeast and Southeast Asia, separately, and analyses based on annual and seasonal
470 median pattern (Figures S15 and S16). Data is available from 1995 to 2022, therefore recent decade
471 situation (e.g., the outbreak of Coronavirus disease 2019) probably affects the trend result. In spite of
472 this condition, generally we can see increasing trends of tropospheric ozone in East Asia, consistent
473 with previous reports (Wang et al., 2019; Lee et al., 2021; Li, S. et al., 2023). Compare to trends in
474 Northeast Asia, it seems that the increasing trend in Southeastern Asia looks more evident. In particular,

ozone trends in Southeast Asia shows high certainty from the surface to ~ 8km consistently (Figure S16). In contrast to the continuous ozone increase in Northeast Asia, however, it seems that the ozone increase in Southeast Asia became weaker recently (Figure S17), requiring the necessity to put on our eye constantly in the future. Seasonal median trends are usually similar to annual trends except winter (DJF). Wintertime trends at Northeast Asia are partly negative in the upper troposphere (different from consistent increasing trends in other seasons), and not evident near the surface (different from increasing trends with high and medium certainty in other seasons). In Southeast Asia, wintertime ozone trends are still increasing, but mostly not evident, different from increasing trends with high certainty in other seasons.

5. Implications for ozone control

Our results reveal significant spatial and seasonal ozone variations over East Asia and Southeast Asia. Spatially, ozone levels are closely associated with anthropogenic emissions (e.g., NO_x emissions), with high ozone concentrations aligning well with the estimated NO_x emission patterns. Figure 16 shows the bottom-up NO_x emissions and the satellite-derived NO₂ columns over East Asia and Southeast Asia. Seasonally, ozone variations are primarily influenced by meteorological conditions and biomass burning emissions in Southeast Asia. For example, ozone peaks usually occur in northern China during summer, in the Pearl River Delta during autumn, and in Southeast Asia during spring.

Relative to East Asia, although the health risks in Southeast Asia tend to be low under short-term ozone exposure metrics (e.g., 95th percentile MDA8 ozone), ozone exceedance days are still notable if WHO standard is applied. The diverse short-term ozone air quality standards in Southeast Asian countries (Figure 3) suggest a great challenge to call for regional joint ozone control. Moreover, the WHO newly introduced peak season ozone concentration standard indicates that both East Asia and Southeast Asia are faced with a widespread risk of long-term ozone exposure, with the vast majority of the region exceeding the WHO standard. In addition to health impacts, the pervasive ozone pollution in East Asia and Southeast Asia is also threatening global food security by its accounting for over 60% of global rice yield (Feng et al. 2022; Yuan et al., 2022). For example, the year-around mean MDA8 ozone over 40 nmol mol⁻¹ over Southeast Asia suggests the high ozone exposure over a threshold of 40 nmol mol⁻¹ (AOT40) that is commonly used to investigate ozone effects on vegetation yield (Feng et al. 2022).

The long-term trend of surface ozone indicates that, based on the available data, high-emission regions

505 in South Korea, Southeast Asia, and China have generally experienced an increase in ozone levels
506 since 2005. However, since 2013, the increase in ozone levels in China has significantly accelerated,
507 while the ozone trends in Thailand and Malaysia in Southeast Asia show no significant changes.
508 Therefore, it is still urgent to attribute the varying ozone trends in East Asia and Southeast Asia across
509 different seasons over the past decade.

510 In the troposphere, the available ozonesonde and IAGOS measurements not only demonstrate the high
511 background ozone in warm seasons over Northeast Asia, but also show an overall increasing tendency
512 in the past three decades. While the increase in tropospheric ozone can be largely attributed to the
513 increased anthropogenic emissions as demonstrated in our companion paper (Lu et al., 2024), the
514 origin of high seasonal background ozone in Northeast Asia remains unclear. Recent studies provide
515 some observational and modeling evidence of stratospheric intrusion (Chen et al., 2024; Columbi et
516 al., 2023) to explain this high background ozone, but a quantitative assessment is urgently needed. In
517 particular, the recent ASIA-AQ campaign (<https://espo.nasa.gov/asia-aq>) flying across Asia countries
518 would be important to understand the high tropospheric ozone issue over East Asia and Southeast Asia.

519

520 **6. Conclusions**

521 Under the framework of the TOAR II (2020-2024) that aims to estimate global and regional
522 tropospheric ozone pollution and its historical trend, in this study we present the most comprehensive
523 view of ozone distributions and evolution over East Asia and Southeast Asia across different
524 spatiotemporal scales in the past two decades. This is done by taking advantage of the available surface
525 ozone measurement in the past two decades (2005-2021) over eight countries, and ten ozonesonde and
526 in-service aircraft measurements within this region. The key conclusions are as follows:

527 Firstly, there are significant spatial and seasonal ozone variations at the present-day level. In summer,
528 seasonal mean MDA8 ozone averaged over 2017-2021 varies from 30 nmol mol⁻¹ in Southeast Asia to
529 over 75 nmol mol⁻¹ in summer in North China and Seoul. Southeast Asia in winter and spring has high
530 mean ozone of 60 nmol mol⁻¹ in Thailand. The seasonality of the 95th percentile ozone resembles the
531 mean ozone evolution, but the widespread occurrence of the very high 95th percentile ozone of over
532 85 nmol mol⁻¹ highlights the severity of ozone pollution. If the WHO standard is applied for short-
533 term exposure, a large fraction the sites will have more than 100 days with MDA8 ozone exceedance.
534 In terms of long-term exposure, the WHO newly-introduced peak season ozone standard indicates that
535 both East Asia and Southeast Asia are faced with a widespread risk of long-term ozone exposure.

536 Secondly, the surface ozone increase in the past two decades is widespread. In particular, South Korea
537 has a national ozone increase with high certainty across different seasons. In Thailand, there is an
538 overall increasing trend in surface ozone but with spatial heterogeneity over 2005-2021. In China, the
539 compiled 11 individual measurements show an overall ozone increase in high-emission regions and at
540 a global baseline station. However, the observed national surface ozone increase in South Korea and
541 Southeast Asia from 2005 is leveling off or even decreased in the past decade (2013-2021), while
542 ozone increase in 2000s over China has amplified after 2013. Surface ozone trends in Japan and
543 Mongolia are generally flat in the past decade.

544 Thirdly, in the troposphere, the high ozone levels in spring and summer at Beijing, Pohang, Sapporo,
545 and Tsukuba site are driven by strong photochemical ozone production and stratospheric ozone
546 intrusion, supported by both the ozonesonde and IAGOS measurements. The difference in tropospheric
547 ozone level between East Asia and Southeast Asia is likely due to the high background ozone from
548 stratospheric intrusion over Northeast Asia. In terms of ozone trends, from a three-decade perspective,
549 the available ozonesonde and aircraft measurements show an overall increasing tendency at different
550 altitudes but feature with strong site-by-site differences. Due to measurement availability, ozone trend
551 in the past decade is still unquantified.

552 Fourthly, the significant spatial ozone variations over East Asia and Southeast Asia are closely
553 associated with anthropogenic emissions, supported by ground-based and satellite measurements. Our
554 study also shows that there is a very high ozone climate penalty over East Asia and Southeast Asia,
555 and the widespread high ozone-temperature slope of 3-8 nmol mol⁻¹ °C⁻¹ persists all the year around
556 in Southeast Asia. More importantly, the observed 95th percentile regression shows a notably increased
557 ozone-temperature slope over Southeast Asia, suggesting a critical issue in future ozone controls.

558

559

560

561

562

Data availability. The sources for all data used in this study, including the observations, meteorological reanalysis and emission data will be provided upon the publication of the manuscript.

Supplement. The supplement related to this article is available online.

Author contributions. K.L. and J.H.K. led and organized the project, working as the co-leads of the East Asia Working Group of Tropospheric Ozone Assessment Report Phase II (TOAR II) with X.L. and T.N. S.J.F., J.Q.Z., X.P.L., L.K.X., J.M.X., Y.X.G., Z.Q.M., M.T.L., T.A., J.G., M.H.L., J.B., J.K., J.H.K., X.L., and T.N. assisted in preparation of observational data. K.L., R.T., W.H.Q., and J.H.K. conducted the analysis and prepared the figures. T.L., Y.F.W., D.Y.T.Z., M.L.T., W.Q.Z. contributed to preparing the figures. K.L. and J.H.K. led the writing of the manuscript. All authors contributed to improving the manuscript.

Competing interests. Some authors are members of the editorial board of Atmospheric Chemistry and Physics.

Acknowledgements. We greatly thank the China's Ministry of Ecology and Environment, Korean Ministry of Environment, National Institute for Environmental Studies, Malaysia Department of Environment, Thailand Pollution Control Department, the Acid Deposition Monitoring Network in East Asia (EANET), World Ozone and Ultraviolet Radiation Data Centre (WOUDC), and In-service Aircraft for a Global Observing System (IAGOS) for running the ozone observation networks. MOZAIC/CARIBIC/IAGOS data were created with support from the European Commission, national agencies in Germany (BMBF), France (MESR), and the UK (NERC), and the IAGOS member institutions (<http://www.iagos.org/partners>). The participating airlines (Lufthansa, Air France, Austrian, China Airlines, Hawaiian Airlines, Air Canada, Iberia, Eurowings Discover, Cathay Pacific, Air Namibia, Sabena) supported IAGOS by carrying the measurement equipment free of charge since 1994. The data are available at <http://www.iagos.fr> thanks to additional support from AERIS. We also thank the previous and current TOAR Steering Committee members (Owen Cooper, Lin Zhang, and Keding Lu) for effortless support of guiding the East Asia Working Group of Tropospheric Ozone Assessment Report Phase II (TOAR II), and the SHADOZ team (Anne M. Thompson, Ryan M. Stauffer and Debra E. Kollonige) for their remarkable contribution to the database of long-term ozone profile measurements.

Financial support. This research was supported by the National Natural Science Foundation of China

(grants 42293323, 42205114, and 42293321), the Natural Science Foundation of Jiangsu Province (BK20240035). This work was also supported by the National Research Foundation of Korea (NRF) grant funded by the Korea government (MSIT) (RS-2023-00219830).

Reference

- Ahamad, F., Griffiths, P. T., Latif, M. T., Juneng, L., and Xiang, C. J.: Ozone Trends from Two Decades of Ground Level Observation in Malaysia, *Atmosphere*, 11, 10.3390/atmos11070755, 2020.
- Ashfold, M. J., Latif, M. T., Mokhtar, A. M., Samah, A. A., Mead, M. I., and Harris, N.: The Relationship between Ozone and Temperature in Greater Kuala Lumpur, Malaysia. *Aerosol Air Qual. Res.*, 24, 240072, 2024.
- Bak, J., Song, E. J., Lee, H. J., Liu, X., Koo, J. H., Kim, J., Jeon, W., Kim, J. H., and Kim, C. H.: Temporal variability of tropospheric ozone and ozone profiles in the Korean Peninsula during the East Asian summer monsoon: insights from multiple measurements and reanalysis datasets, *Atmos. Chem. Phys.*, 22, 14177-14187, 10.5194/acp-22-14177-2022, 2022.
- Cao, T. H., Wang, H. C., Li, L., Lu, X., Liu, Y. M., and Fan, S. J.: Fast spreading of surface ozone in both temporal and spatial scale in Pearl River Delta, *J. Environ. Sci.*, 137, 540-552, 10.1016/j.jes.2023.02.025, 2024.
- Chang, K. L., Petropavlovskikh, I., Cooper, O. R., Schultz, M. G., and Wang, T.: Regional trend analysis of surface ozone observations from monitoring networks in eastern North America, Europe and East Asia, *Elementa*, 5, 10.1525/elementa.243, 2017.
- Cheesman, A. W., Brown, F., Artaxo, P., Farha, M. N., Folberth, G. A., Hayes, F. J., Heinrich, V. H. A., Hill, T. C., Mercado, L. M., Oliver, R. J., O' Sullivan, M., Uddling, J., Cernusak, L. A., and Sitch, S.: Reduced productivity and carbon drawdown of tropical forests from ground-level ozone exposure, *Nat. Geosci.* 17, 10.1038/s41561-024-01530-1, 2024.
- Chen, Z. X., Liu, J. N., Qie, X. S., Cheng, X. G., Yang, M. M., Shu, L., and Zang, Z.: Stratospheric influence on surface ozone pollution in China, *Nat. Commun.*, 15, 10.1038/s41467-024-48406-x, 2024.
- Chen, Z. X., Liu, J. N., Qie, X. S., Cheng, X. G., Shen, Y. K., Yang, M. M., Jiang, R. B., and Liu, X. K.: Transport of substantial stratospheric ozone to the surface by a dying typhoon and shallow convection, *Atmos. Chem. Phys.*, 22, 8221-8240, 10.5194/acp-22-8221-2022, 2022.
- Colombi, N. K., Jacob, D. J., Yang, L. H., Zhai, S., Shah, V., Grange, S. K., Yantosca, R. M., Kim, S., and Liao, H.: Why is ozone in South Korea and the Seoul metropolitan area so high and increasing?, *Atmos. Chem. Phys.*, 23, 4031-4044, 10.5194/acp-23-4031-2023, 2023.
- DeLang, M.N., Becker, J.S., Chang, K.L., Serre, M.L., Cooper, O.R., Schultz, M.G., Schröder, S., Lu, X., Zhang, L., Deushi, M. and Josse, B.: Mapping yearly fine resolution global surface ozone through the Bayesian maximum entropy data fusion of observations and model output for 1990–2017. *Environ. Sci. Tech.*, 55(8), 4389-4398, 2021.
- Feng, Z. Z., Xu, Y. S., Kobayashi, K., Dai, L. L., Zhang, T. Y., Agathokleous, E., Calatayud, V., Paoletti, E., Mukherjee, A., Agrawal, M., Park, R. J., Oak, Y. J., and Yue, X.: Ozone pollution threatens the production of major staple crops in East Asia, *Nat. Food*, 3, 47-+, 10.1038/s43016-021-00422-6,

2022.

Gopikrishnan, G. S. and Kuttippurath, J.: Global tropical and extra-tropical tropospheric ozone trends and radiative forcing deduced from satellite and ozonesonde measurements for the period 2005–2020. *Environ. Pollut.*, 361, 124869, 10.1016/j.envpol.2024.124869, 2024.

Gu, Y. X., Li, K., Xu, J. M., Liao, H., and Zhou, G. Q.: Observed dependence of surface ozone on increasing temperature in Shanghai, China, *Atmos. Environ.*, 221, 10.1016/j.atmosenv.2019.117108, 2020.

Jiang, Z. J., Li, J., Lu, X., Gong, C., Zhang, L., and Liao, H.: Impact of western Pacific subtropical high on ozone pollution over eastern China, *Atmos. Chem. Phys.*, 21, 2601-2613, 10.5194/acp-21-2601-2021, 2021.

Kawano, N., Nagashima, T., and Sugata, S.: Changes in seasonal cycle of surface ozone over Japan during 1980-2015, *Atmos. Environ.*, 279, 10.1016/j.atmosenv.2022.119108, 2022.

Kim, S. W., Kim, K. M., Jeong, Y., Seo, S., Park, Y., and Kim, J.: Changes in surface ozone in South Korea on diurnal to decadal timescales for the period of 2001-2021, *Atmos. Chem. Phys.*, 23, 12867-12886, 10.5194/acp-23-12867-2023, 2023.

Lee, H. J., Chang, L. S., Jaffe, D. A., Bak, J., Liu, X., Abad, G. G., Jo, H. Y., Jo, Y. J., Lee, J. B., and Kim, C. H.: Ozone Continues to Increase in East Asia Despite Decreasing NO₂: Causes and Abatements, *Remote Sens.*, 13, 10.3390/rs13112177, 2021.

Lee, H. M. and Park, R. J.: Factors determining the seasonal variation of ozone air quality in South Korea: Regional background versus domestic emission contributions, *Environ. Pollut.*, 308, 10.1016/j.envpol.2022.119645, 2022.

Li, F., Zheng, Q. P., Jiang, Y. C., Xun, A. P., Zhang, J. R., Zheng, H., and Wang, H.: Impact analysis of super Typhoon 2114 'Chanthu' on the air quality of coastal cities in southeast China based on multi-source measurements, *Atmosphere*, 14, 10.3390/atmos14020380, 2023a.

Li, K., Jacob, D. J., Liao, H., Shen, L., Zhang, Q., and Bates, K. H.: Anthropogenic drivers of 2013-2017 trends in summer surface ozone in China, *Proc. Nat. Acad. Sci.*, 116, 422-427, 10.1073/pnas.1812168116, 2019.

Li, K., Jacob, D. J., Shen, L., Lu, X., De Smedt, I., and Liao, H.: Increases in surface ozone pollution in China from 2013 to 2019: anthropogenic and meteorological influences, *Atmos. Chem. Phys.*, 20, 11423-11433, 10.5194/acp-20-11423-2020, 2020.

Li, K., Jacob, D. J., Liao, H., Qiu, Y. L., Shen, L., Zhai, S. X., Bates, K. H., Sulprizio, M. P., Song, S. J., Lu, X., Zhang, Q., Zheng, B., Zhang, Y. L., Zhang, J. Q., Lee, H. C., and Kuk, S. K.: Ozone pollution in the North China Plain spreading into the late-winter haze season, *Proc. Nat. Acad. Sci.*, 118, 10.1073/pnas.2015797118, 2021.

Li, M., Kurokawa, J., Zhang, Q., Woo, J. H., Morikawa, T., Chatani, S., Lu, Z., Song, Y., Geng, G., Hu, H., Kim, J., Cooper, O. R., and McDonald, B. C.: MIXv2: a long-term mosaic emission inventory for Asia (2010–2017), *Atmos. Chem. Phys.*, 24, 3925-3952, 10.5194/acp-24-3925-2024, 2024.

Li, S., Yang, Y., Wang, H. L., Li, P. W., Li, K., Ren, L. L., Wang, P. Y., Li, B. J., Mao, Y. H., and Liao, H.: Rapid increase in tropospheric ozone over Southeast Asia attributed to changes in precursor emission source regions and sectors, *Atmos. Environ.*, 304, 10.1016/j.atmosenv.2023.119776, 2023b.

Liao, Z. H., Ling, Z. H., Gao, M., Sun, J. R., Zhao, W., Ma, P. K., Quan, J. N., and Fan, S. J.: Tropospheric Ozone Variability Over Hong Kong Based on Recent 20 years (2000-2019) Ozonesonde Observation, *J. Geophys. Res. Atmos.*, 126, 10.1029/2020jd033054, 2021.

- Lu, X., Zhang, L., Wang, X. L., Gao, M., Li, K., Zhang, Y. Z., Yue, X., and Zhang, Y. H.: Rapid Increases in Warm-Season Surface Ozone and Resulting Health Impact in China Since 2013, *Environ. Sci. Tech. Lett.*, 7, 240-247, 10.1021/acs.estlett.0c00171, 2020.
- Lu, X., Hong, J. Y., Zhang, L., Cooper, O. R., Schultz, M. G., Xu, X. B., Wang, T., Gao, M., Zhao, Y. H., and Zhang, Y. H.: Severe Surface Ozone Pollution in China: A Global Perspective, *Environ. Sci. Tech. Lett.*, 5, 487-494, 10.1021/acs.estlett.8b00366, 2018.
- Lu, X., Liu, Y., Su, J., Weng, X., Ansari, T., Zhang, Y., He, G., Zhu, Y., Wang, H., Zeng, G., Li, J., He, C., Li, S., Amnuaylojaroen, T., Butler, T., Fan, Q., Fan, S., Forster, G. L., Gao, M., Hu, J., Kanaya, Y., Latif, M. T., Lu, K., Nédélec, P., Nowack, P., Sauvage, B., Xu, X., Zhang, L., Li, K., Koo, J.-H., and Nagashima, T.: Tropospheric ozone trends and attributions over East and Southeast Asia in 1995–2019: An integrated assessment using statistical methods, machine learning models, and multiple chemical transport models, *EGUsphere*, 10.5194/egusphere-2024-3702, 2024.
- Lyu, X., Li, K., Guo, H., Morawska, L., Zhou, B. N., Zeren, Y., Jiang, F., Chen, C. H., Goldstein, A. H., Xu, X. B., Wang, T., Lu, X., Zhu, T., Querol, X., Chatani, S., Latif, M. T., Schuch, D., Sinha, V., Kumar, P., Mullins, B., Seguel, R., Shao, M., Xue, L. K., Wang, N., Chen, J. M., Gao, J., Chai, F. H., Simpson, I., Sinha, B., and Blake, D. R.: A synergistic ozone-climate control to address emerging ozone pollution challenges, *One Earth*, 6, 964-977, 10.1016/j.oneear.2023.07.004, 2023.
- Kang, H., H.-G. Kim, J. Kim, T. Lee, J.-H. Koo, S.-S. Park, Y. Choi, W.-J. Lee, S. A. Shin, and J. Park, Atmospheric and Ozone Profiling Data Measured with Ozone sonde from 2021 to 2024, *GEO DATA*, 6(4), 561-577, <https://doi.org/10.22761/GD.2024.0041>, 2024. (written in Korean)
- Ma, Z., Xu, J., Quan, W., Zhang, Z., Lin, W., and Xu, X.: Significant increase of surface ozone at a rural site, north of eastern China. *Atmos. Chem. Phys.*, 16(6), 3969-3977, 2016.
- Nagashima, T., Sudo, K., Akimoto, H., Kurokawa, J., and Ohara, T.: Long-term change in the source contribution to surface ozone over Japan, *Atmos. Chem. Phys.*, 17, 8231-8246, 10.5194/acp-17-8231-2017, 2017.
- Neu, J. L., Flury, T., Manney, G. L., Santee, M. L., Livesey, N. J., and Worden, J.: Tropospheric ozone variations governed by changes in stratospheric circulation. *Nat. Geosci.*, 7(5), 340-344, 2014.
- Park, S. S., Kim, J., Cho, H. K., Lee, H., Lee, Y., and Miyagawa, K.: Sudden increase in the total ozone density due to secondary ozone peaks and its effect on total ozone trends over Korea, *Atmos. Environ.*, 47, 226-235, 10.1016/j.atmosenv.2011.11.011, 2012.
- Salvador, C. M. G., Alindajao, A. D., Burdeos, K. B., Lavapie, M. A. M., Yee, J. R., Bautista, A. T., Pabroa, P. C. B., and Capangpangan, R. Y.: Assessment of Impact of Meteorology and Precursor in Long-term Trends of PM and Ozone in a Tropical City, *Aerosol Air Qual. Res.*, 22, 10.4209/aaqr.210269, 2022.
- Sukkhum, S., Lim, A., Ingviya, T., and Saelim, R.: Seasonal Patterns and Trends of Air Pollution in the Upper Northern Thailand from 2004 to 2018, *Aerosol Air Qual. Res.*, 22, 10.4209/aaqr.210318, 2022.
- Sun, L., Xue, L., Wang, T., Gao, J., Ding, A., Cooper, O.R., Lin, M., Xu, P., Wang, Z., Wang, X. and Wen, L.: Significant increase of summertime ozone at Mount Tai in Central Eastern China. *Atmos. Chem. Phys.*, 16(16), 10637-10650, 2016.
- Sun, H. Z., van Daalen, K. R., Morawska, L., Guillas, S., Giorio, C., Di, Q., Kan, H., Loo, E. X.-L., Shek, L. P., Watts, N., Guo, Y., and Archibald, A. T.: An estimate of global cardiovascular mortality burden attributable to ambient ozone exposure reveals urban-rural environmental injustice, *One Earth*, 7, 1803-1819, <https://doi.org/10.1016/j.oneear.2024.08.018>, 2024.
- Vingarzan, R. (2004). A review of surface ozone background levels and trends. *Atmos. Environ.*,

38(21), 3431-3442, 2004.

Wang, H., Lu, X., Palmer, P. I., Zhang, L., Lu, K., Li, K., Nagashima, T., Koo, J.-H., Tanimoto, H., Wang, H., Gao, M., He, C., Wu, K., Fan, S., and Zhang, Y.: Deciphering decadal urban ozone trends from historical records since 1980, *Natl. Sci. Rev.*, 11, 10.1093/nsr/nwae369, 2024.

Wang, H. L., Lu, X., Jacob, D. J., Cooper, O. R., Chang, K. L., Li, K., Gao, M., Liu, Y. M., Sheng, B. S., Wu, K., Wu, T. W., Zhang, J., Sauvage, B., Nédélec, P., Blot, R., and Fan, S. J.: Global tropospheric ozone trends, attributions, and radiative impacts in 1995-2017: an integrated analysis using aircraft (IAGOS) observations, ozonesonde, and multi-decadal chemical model simulations, *Atmos. Chem. Phys.*, 22, 13753-13782, 10.5194/acp-22-13753-2022, 2022b.

Wang, T., Dai, J. N., Lam, K. S., Nan Poon, C., and Brasseur, G. P.: Twenty-Five Years of Lower Tropospheric Ozone Observations in Tropical East Asia: The Influence of Emissions and Weather Patterns, *Geophys. Res. Lett.*, 46, 11463-11470, 10.1029/2019gl084459, 2019.

Wang, X. L., Fu, T. M., Zhang, L., Lu, X., Liu, X., Amnuaylojaroen, T., Latif, M. T., Ma, Y. P., Zhang, L. J., Feng, X., Zhu, L., Shen, H. Z., and Yang, X.: Rapidly Changing Emissions Drove Substantial Surface and Tropospheric Ozone Increases Over Southeast Asia, *Geophys. Res. Lett.*, 49, 10.1029/2022gl100223, 2022a.

Xu, X. B., Lin, W. L., Xu, W. Y., Jin, J. L., Wang, Y., Zhang, G., Zhang, X. C., Ma, Z. Q., Dong, Y. Z., Ma, Q. L., Yu, D. J., Li, Z., Wang, D. D., and Zhao, H. R.: Long-term changes of regional ozone in China: implications for human health and ecosystem impacts, *Elementa*, 8, 10.1525/elementa.409, 2020.

Xue, L., Ding, A., Cooper, O., Huang, X., Wang, W., Zhou, D., Wu, Z., McClure-Begley, A., Petropavlovskikh, I., Andreae, M.O. and Fu, C.: ENSO and Southeast Asian biomass burning modulate subtropical trans-Pacific ozone transport. *Natl. Sci. Rev.*, 8(6), nwaa132, 2021.

Ye, X. P., Zhang, L., Wang, X. L., Lu, X., Jiang, Z. J., Lu, N., Li, D. Y., and Xu, J. Y.: Spatial and temporal variations of surface background ozone in China analyzed with the grid-stretching capability of GEOS-Chem High Performance, *Sci. Total Environ.*, 914, 10.1016/j.scitotenv.2024.169909, 2024.

Yin, Z., Wang, H., Li, Y., Ma, X., and Zhang, X.: Links of climate variability in Arctic sea ice, Eurasian teleconnection pattern and summer surface ozone pollution in North China. *Atmos. Chem. Phys.*, 19(6), 3857-3871, 2019.

Yuan, S., Stuart, A.M., Laborte, A.G., Rattalino Edreira, J.I., Dobermann, A., Kien, L.V.N., Thúy, L.T., Paothong, K., Traesang, P., Tint, K.M. and San, S.S.: Southeast Asia must narrow down the yield gap to continue to be a major rice bowl. *Nat. Food*, 3(3), 217-226, 2022.

Zanis, P., Akritidis, D., Turnock, S., Naik, V., Szopa, S., Georgoulas, A.K., Bauer, S.E., Deushi, M., Horowitz, L.W., Keeble, J. and Le Sager, P.: Climate change penalty and benefit on surface ozone: a global perspective based on CMIP6 earth system models. *Environ. Res. Lett.*, 17(2), 024014, 2022.

Zeng, Y. S., Zhang, J. Q., Li, D., Liao, Z. H., Bian, J. C., Bai, Z. X., Shi, H. R., Xuan, Y. J., Yao, Z. D., and Chen, H. B.: Vertical distribution of tropospheric ozone and its sources of precursors over Beijing: Results from ~ 20 years of ozonesonde measurements based on clustering analysis, *Atmos. Res.*, 284, 10.1016/j.atmosres.2023.106610, 2023.

Zhan, C. C. and Xie, M.: Exploring the link between ozone pollution and stratospheric intrusion under the influence of tropical cyclone Ampil, *Sci. Total Environ.*, 828, 10.1016/j.scitotenv.2022.154261, 2022.

Zhang, J., Li, D., Bian, J., Xuan, Y., Chen, H., Bai, Z., Wan, X., Zheng, X., Xia, X. and Lü, D.: Long-

term ozone variability in the vertical structure and integrated column over the North China Plain: results based on ozonesonde and Dobson measurements during 2001–2019. *Environ. Res. Lett.*, 16(7), 074053, 2021.

Zhang, X. Y., Xu, W. Y., Zhang, G., Lin, W. L., Zhao, H. R., Ren, S. X., Zhou, G. S., Chen, J. M., and Xu, X. B.: First long-term surface ozone variations at an agricultural site in the North China Plain: Evolution under changing meteorology and emissions, *Sci. Total Environ.*, 860, 10.1016/j.scitotenv.2022.160520, 2023.

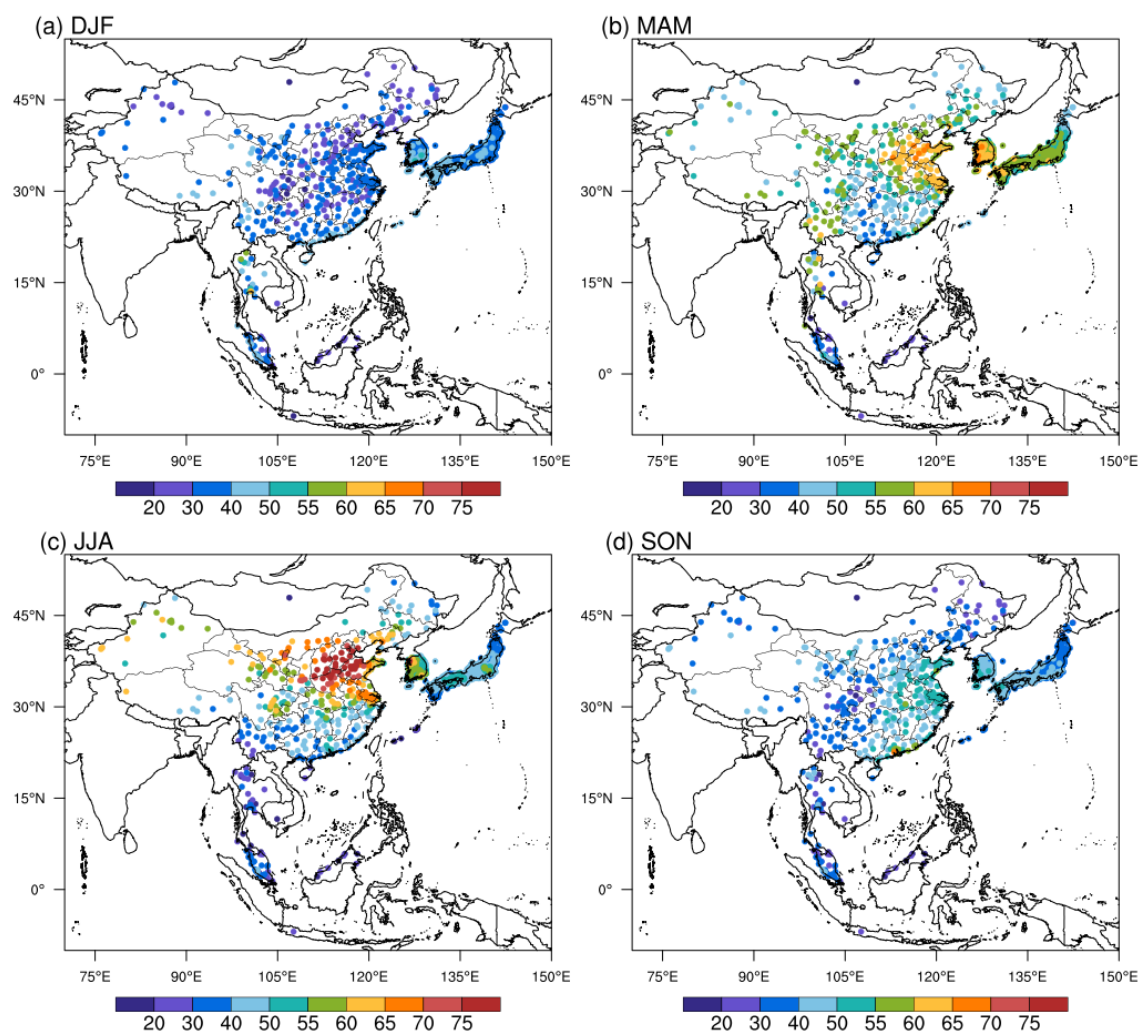
Zhang, Y. N., Xiang, Y. R., Chan, L. Y., Chan, C. Y., Sang, X. F., Wang, R., and Fu, H. X.: Procuring the regional urbanization and industrialization effect on ozone pollution in Pearl River Delta of Guangdong, China. *Atmos. Environ.*, 45(28), 4898–4906, 2011.

Zhao, Z. J. and Wang, Y. X.: Influence of the West Pacific subtropical high on surface ozone daily variability in summertime over eastern China, *Atmos. Environ.*, 170, 197–204, 10.1016/j.atmosenv.2017.09.024, 2017.

Zheng, B., Tong, D., Li, M., Liu, F., Hong, C., Geng, G., Li, H., Li, X., Peng, L., Qi, J., Yan, L., Zhang, Y., Zhao, H., Zheng, Y., He, K., and Zhang, Q.: Trends in China's anthropogenic emissions since 2010 as the consequence of clean air actions, *Atmos. Chem. Phys.*, 18, 14095–14111, 10.5194/acp-18-14095-2018, 2018.

Zhou, H., Yue, X., Dai, H., Geng, G., Yuan, W., Chen, J., Shen, G., Zhang, T., Zhu, J., and Liao, H.: Recovery of ecosystem productivity in China due to the Clean Air Action plan. *Nat. Geosci.*, 17, 1233–1239, 10.1038/s41561-024-01586-z, 2024.

Zhou, Y., Yang, Y., Wang, H., Wang, J., Li, M., Li, H., Wang, P., Zhu, J., Li, K. and Liao, H.: Summer ozone pollution in China affected by the intensity of Asian monsoon systems. *Sci. Total Environ.*, 849, 157785, 2022.



806

807 **Figure 1.** The observed seasonal mean MDA8 ozone (nmol mol^{-1}) in (a) DJF, (b) MAM, (c) JJA, and
808 (d) SON averaged during 2017-2021 over East Asia and Southeast Asia. There are eight countries with
809 surface ozone measurements, including Cambodia (1 site), China (360 sites), Indonesia (1 site), Japan
810 (1187 sites), Malaysia (66 sites), Mongolia (1 site), South Korea (473 sites), and Thailand (25 sites).

811

812

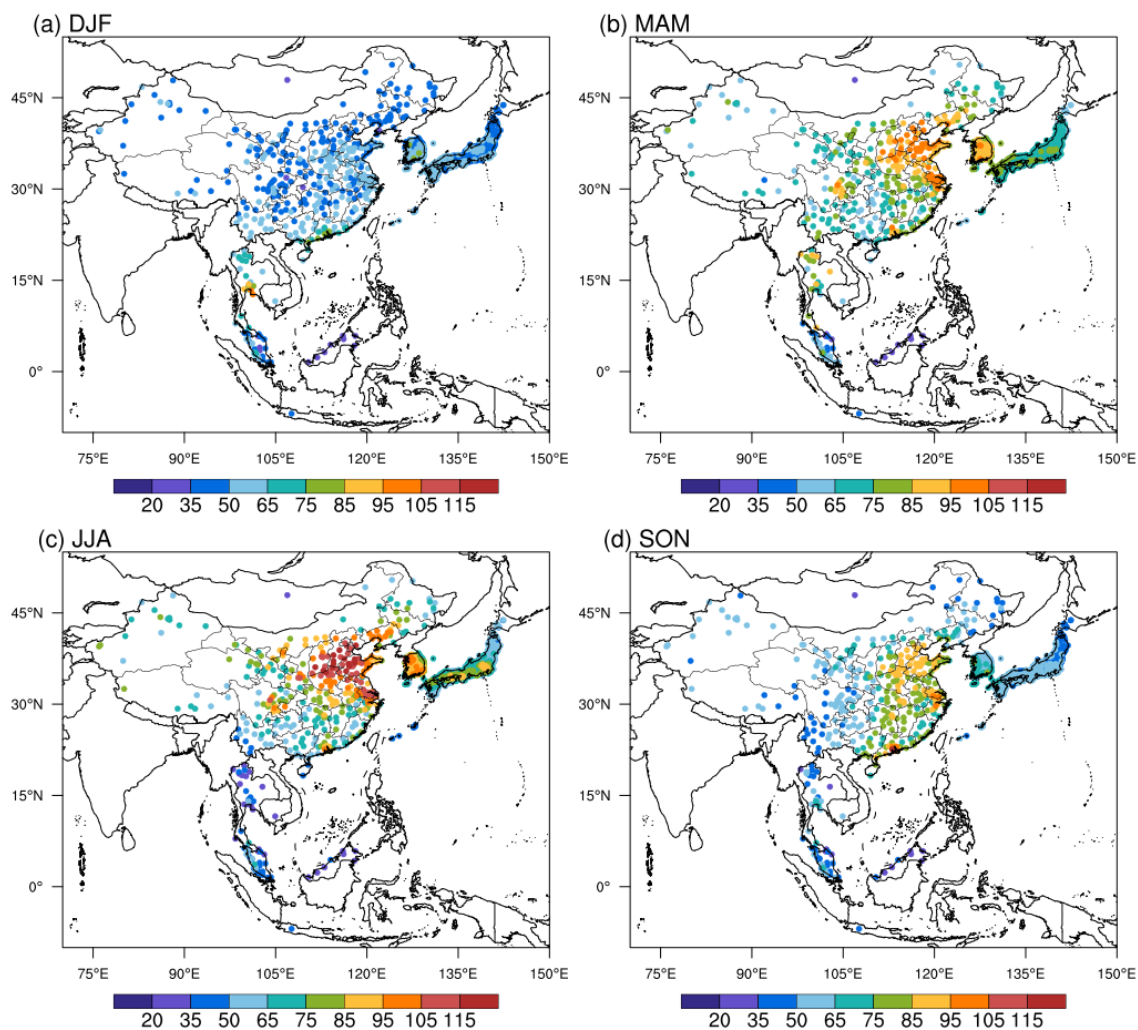


Figure 2. Same as Figure 1 but for the seasonal 95th percentile MDA8 ozone (nmol mol^{-1}) averaged over 2017-2021. This metric represents the extreme high ozone values that are related to short-term ozone exposure.

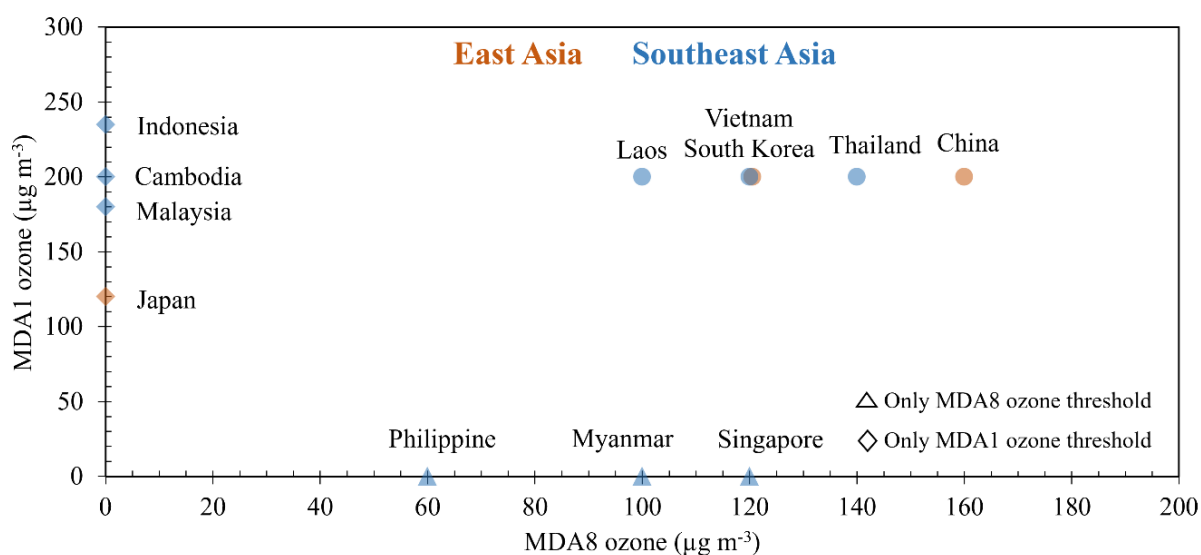


Figure 3. The national ambient ozone air quality standard in East Asia and Southeast Asia. The maximum daily 8 h average (MDA8) and/or maximum daily 1 h average (MDA1) ozone thresholds are routinely adopted but they vary greatly in different countries. The sources for these thresholds are given in Table S2. Under standard conditions (1013 hPa, 273 K), $1 \text{ nmol mol}^{-1} = 2.14 \mu\text{g m}^{-3}$.

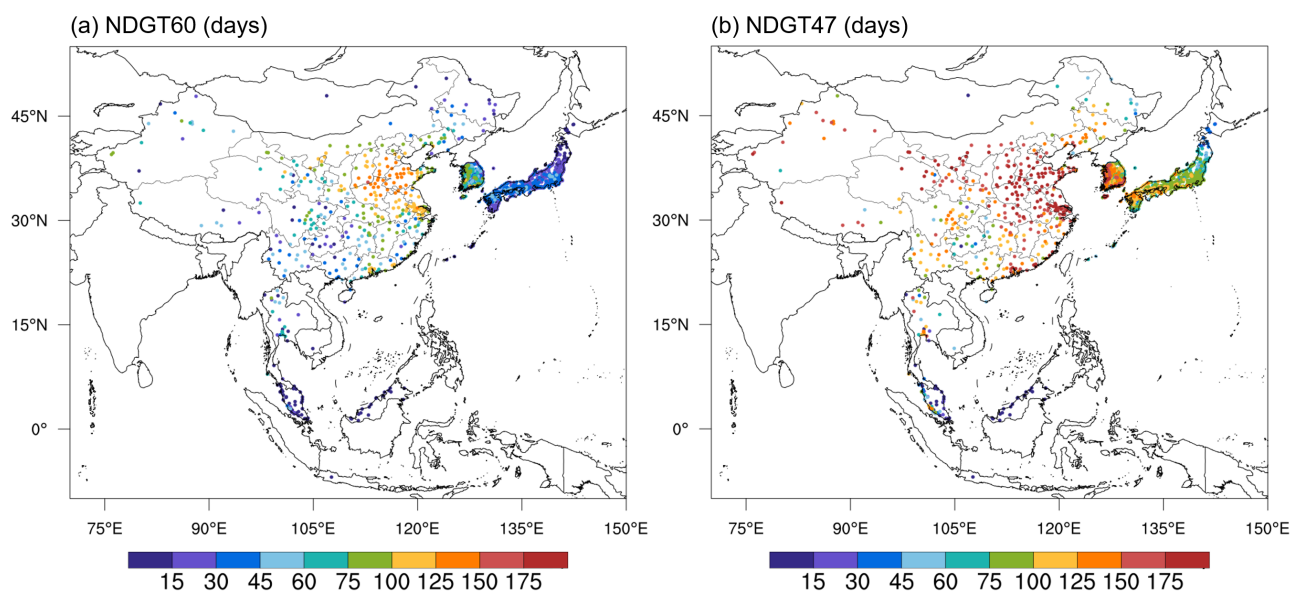


Figure 4. Annual number of days with daily MDA8 ozone greater than 60 nmol mol^{-1} (NDGT60) and greater than the WHO standard of $100 \mu\text{g m}^{-3}$ (NDGT47) averaged over 2017-2021. Under standard conditions (1013 hPa , 273 K), $1 \text{ nmol mol}^{-1} = 2.14 \mu\text{g m}^{-3}$.

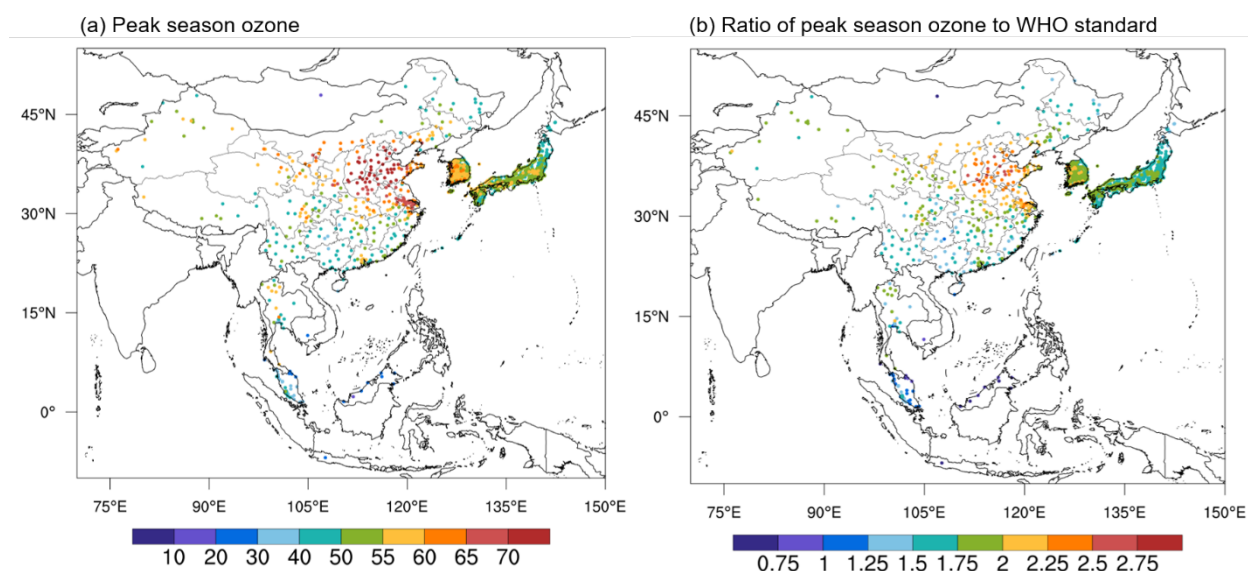


Figure 5. Annual mean peak season ozone (nmol mol⁻¹) averaged over 2017-2021 (a) and the ratio of the observed peak season ozone to the WHO standard of 60 µg m⁻³ (b). As introduced by the WHO, the concentration of peak season ozone is calculated by using the average monthly MDA8 ozone concentration in the six consecutive months with the highest six-month running-average ozone concentration. This new metric represents the long-term ozone exposure.

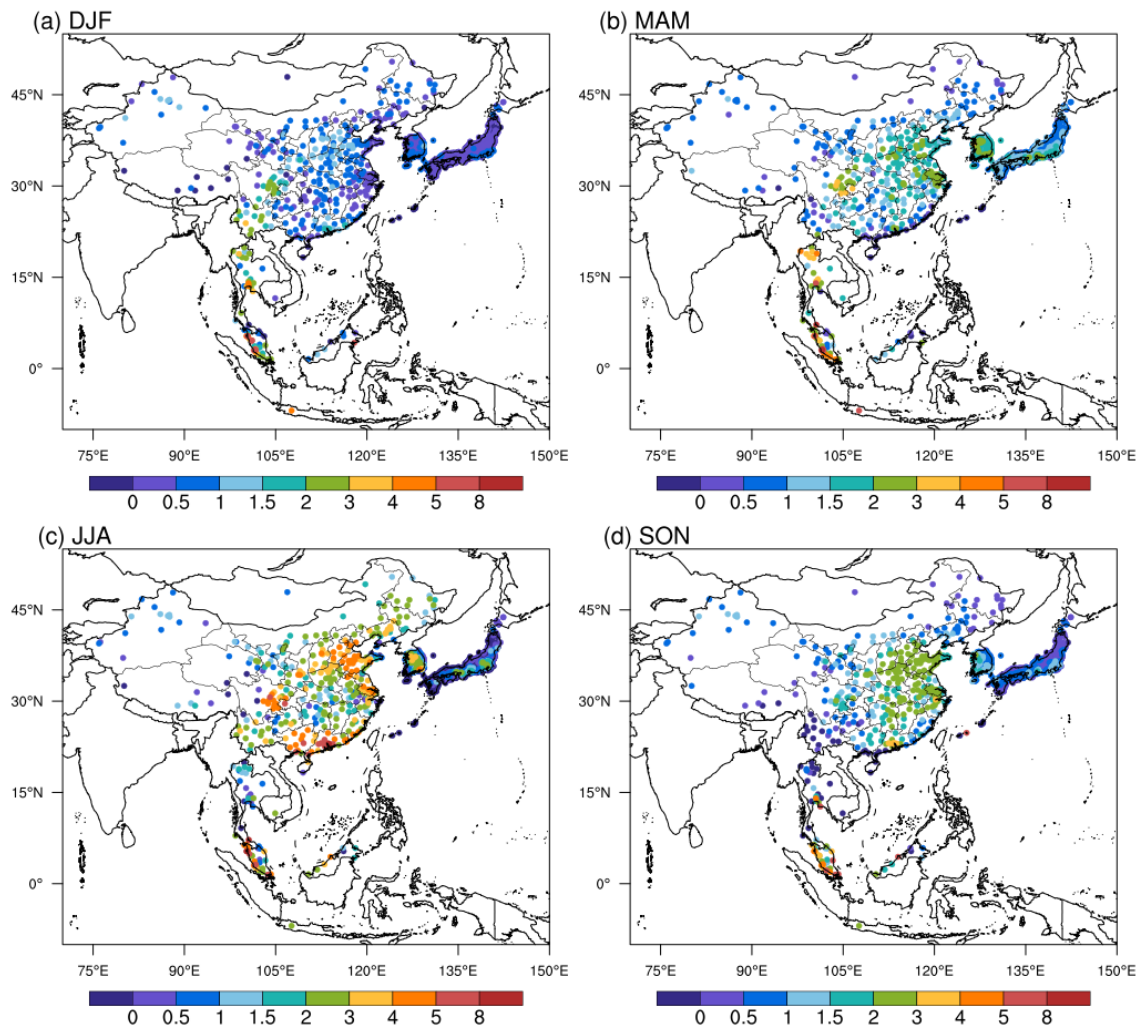


Figure 6. The observed 50th percentile regression slope ($\text{nmol mol}^{-1} \text{ }^{\circ}\text{C}^{-1}$) between daily surface MDA8 ozone and daily maximum 2-m air temperature in (a) DJF, (b) MAM, (c) JJA, and (d) SON averaged over 2017-2021.

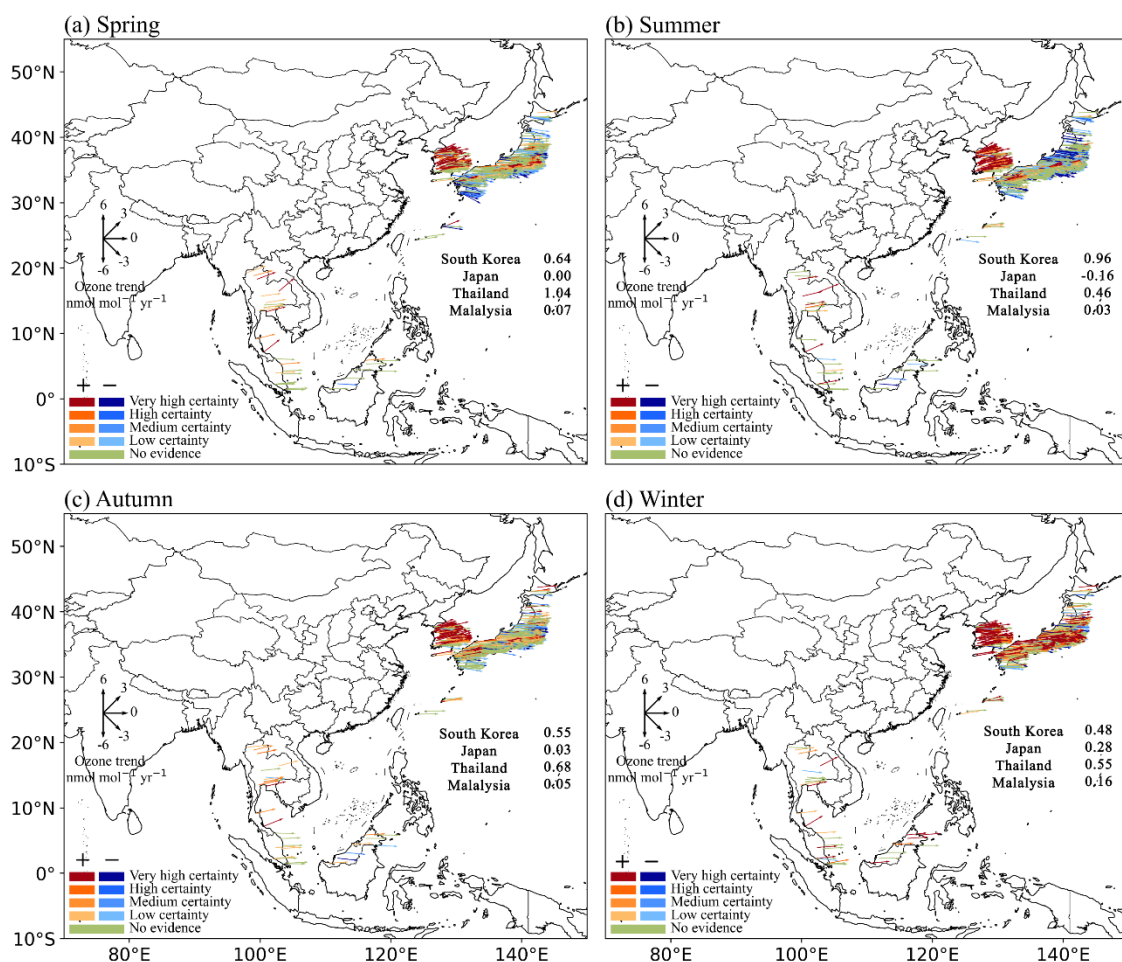


Figure 7. The observed 2005-2021 ozone trends (nmol mol⁻¹ yr⁻¹) during (a) spring, (b) summer, (c) autumn, and (d) winter over East Asia and Southeast Asia. Here it only includes ozone measurements from Malaysia (19 sites), Japan (946 sites), South Korea (226 sites), and Thailand (13 sites). National surface ozone data in China is not available before 2013, therefore not shown in this figure. To follow the trend reliability scale recommended by the TOAR II, here we use “very high certainty” to denote $p \leq 0.01$, “high certainty” to denote $0.05 \geq p > 0.01$, and “medium certainty” to denote $0.10 \geq p > 0.05$; positive trends are in red and negative trends are in blue.

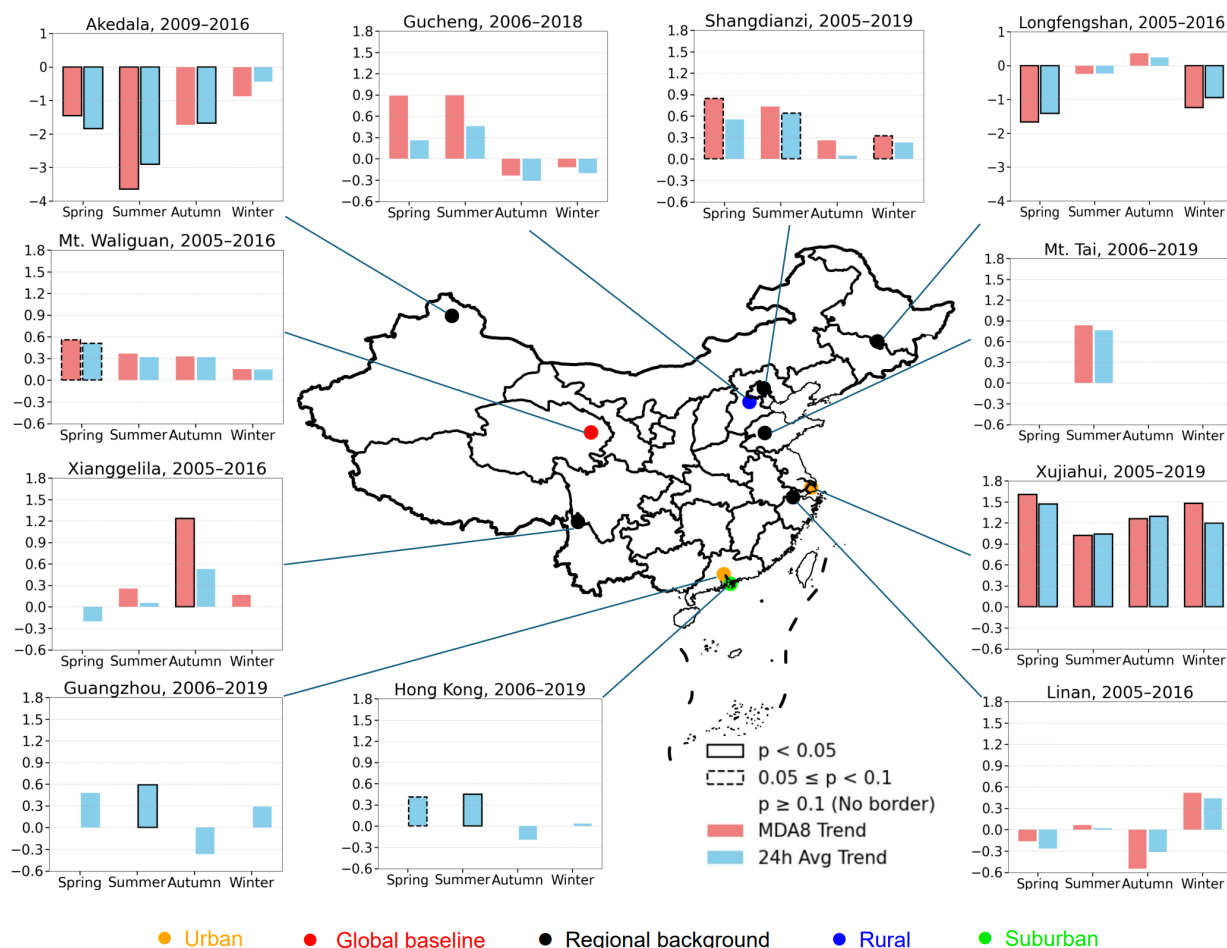


Figure 8. The observed long-term ozone trends (nmol mol⁻¹ yr⁻¹) after 2005 in 11 measurement sites over China. There are 1 global baseline station, 5 regional background stations, 1 rural station, 1 suburban station, and 2 urban stations. Due to data availability, we use the MDA8 ozone and/or 24-hour mean ozone in the calculation of ozone trends. The p value for estimated ozone trends is also highlighted by rectangles.

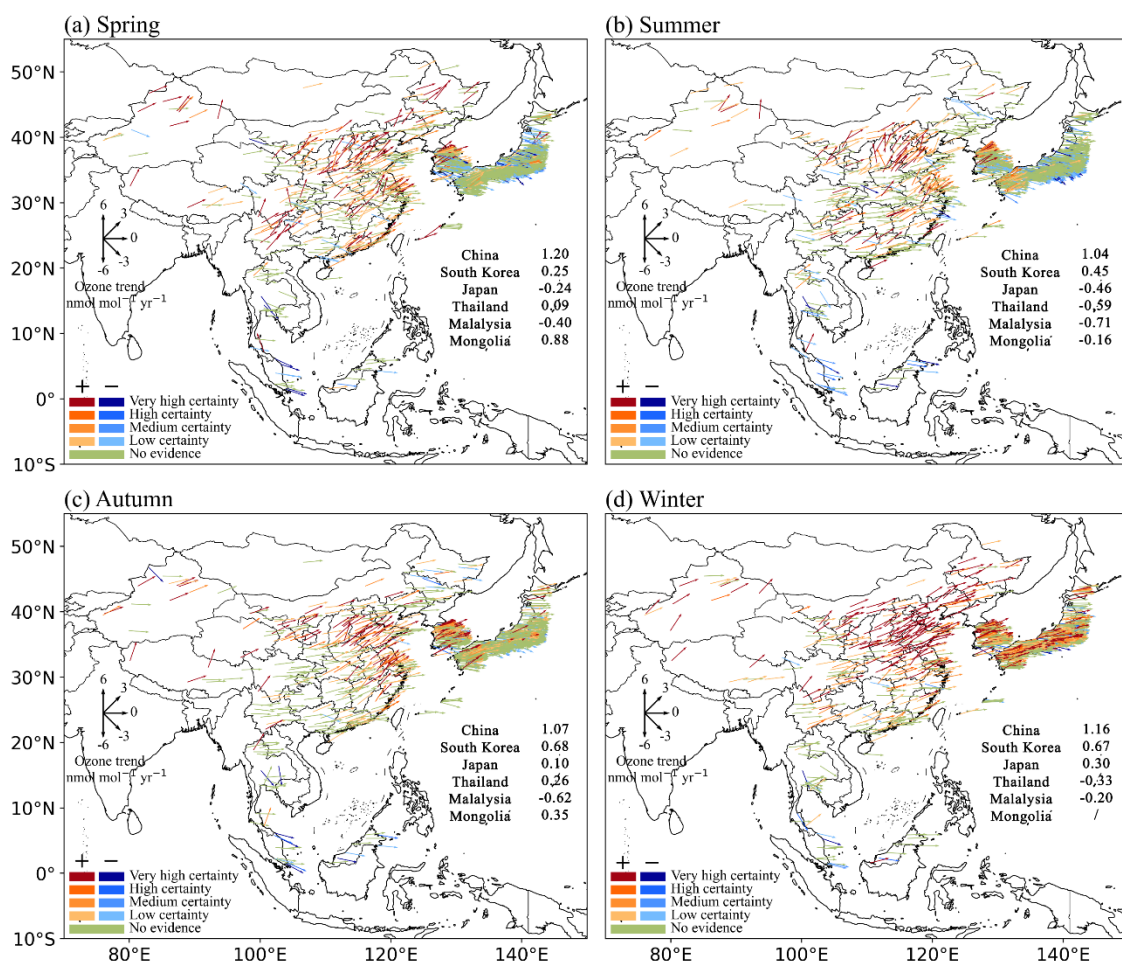


Figure 9. Same with Figure 7 but for the observed 2013-2021 ozone trends ($\text{nmol mol}^{-1} \text{yr}^{-1}$) over East Asia and Southeast Asia. Here it includes ozone measurements from China (335 sites), Malaysia (19 sites), Mongolia (1 site), Japan (1130 sites), South Korea (270 sites), and Thailand (22 sites). To follow the trend reliability scale recommended by the TOAR II, here we use “very high certainty” to denote $p \leq 0.01$, “high certainty” to denote $0.05 \geq p > 0.01$, and “medium certainty” to denote $0.10 \geq p > 0.05$; positive trends are in red and negative trends are in blue.

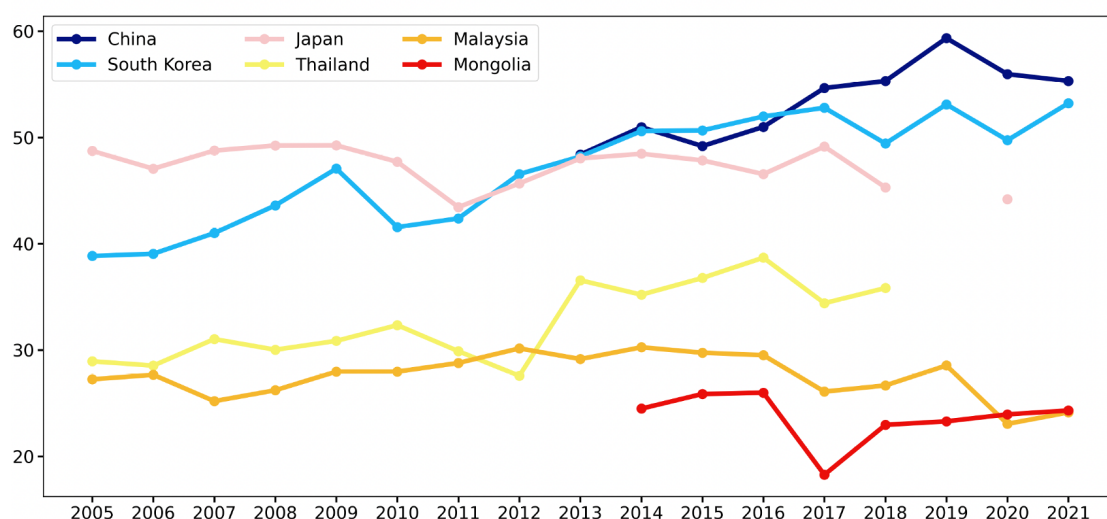


Figure 10. The observed national mean MDA8 ozone (nmol mol^{-1}) during warm seasons (April to September) from 2005 to 2021 in East Asia and Southeast Asia.

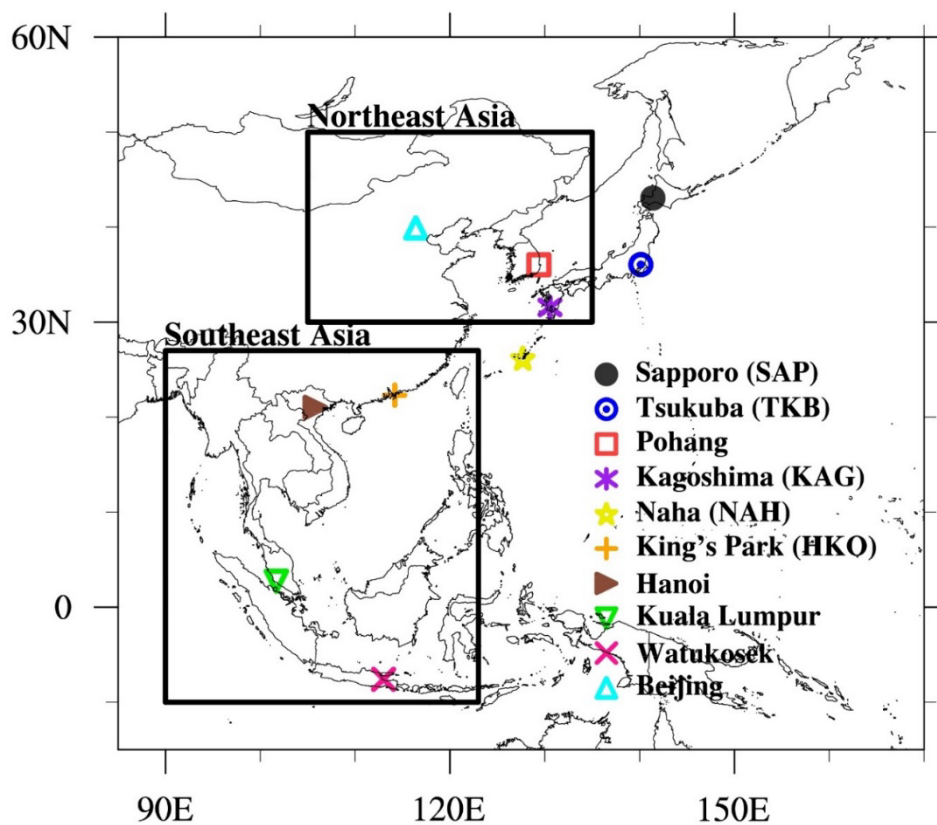


Figure 11. Map showing the location of ozonesonde sites (symbols) and the coverage of the IAGOS measurements (black box) considered in this study.

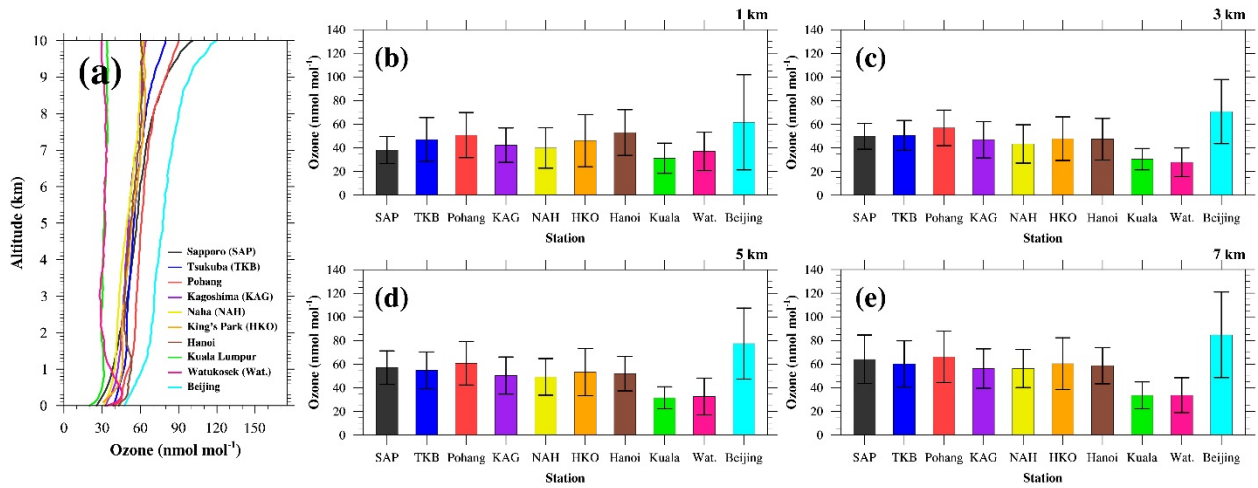


Figure 12. (a) Climatological mean vertical ozone profiles of 10 ozonesonde sites in the troposphere (from 0 to 10 km altitude) are compared. Also, mean ozone mixing ratio values of 10 ozonesonde sites at (b) 1 km, (c) 3 km, (d) 5 km, and (e) 7 km altitude are compared. Error-bar shows the 1-sigma standard deviation range. The number in the parenthesis in panel (a) indicates the number of used data for each site.

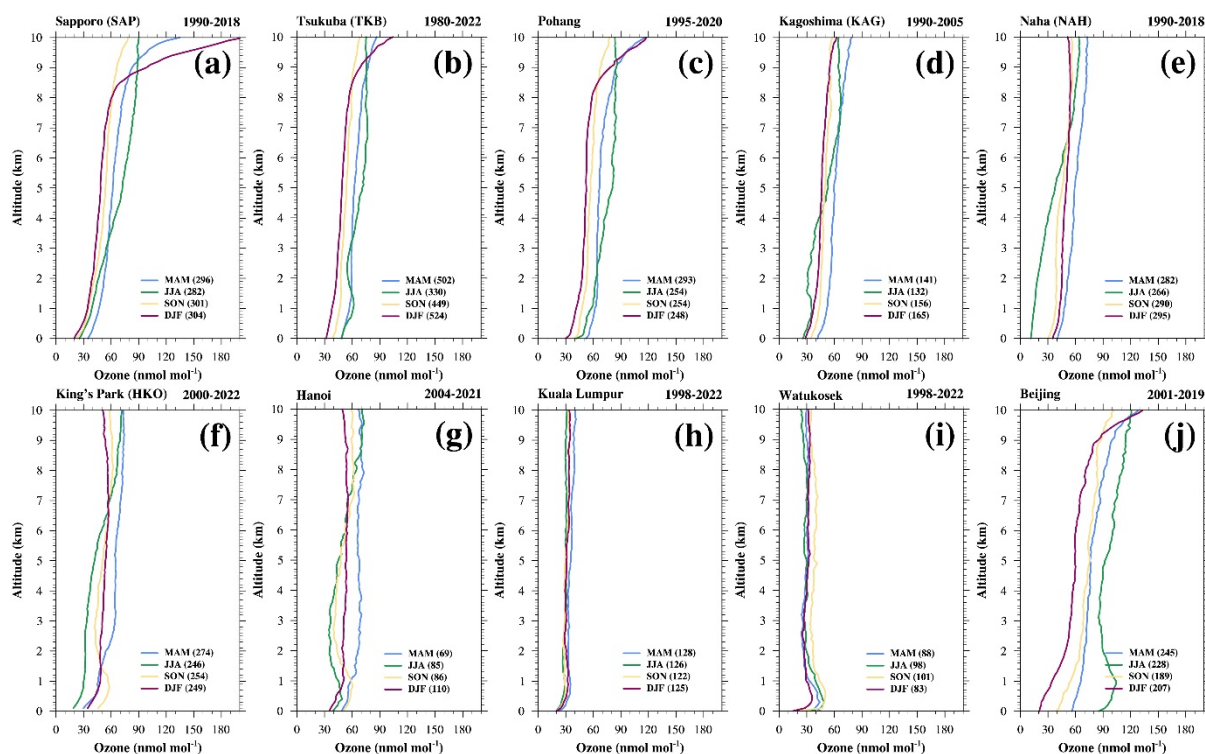


Figure 13. Seasonal mean vertical ozone profiles at (a) Sapporo, (b) Tsukuba, (c) Pohang, (d) Kagoshima, (e) Naha, (f) King's park, (g) Hanoi, (h) Kuala Lumpur, (i) Watukosek, and (j) Beijing site: March-April-May (MAM, blue), June-July-August (JJA, green), September-October-November (SON, orange), and December-January-February (DJF, red). The number in the parenthesis of each panel indicates the number of used data for each season.

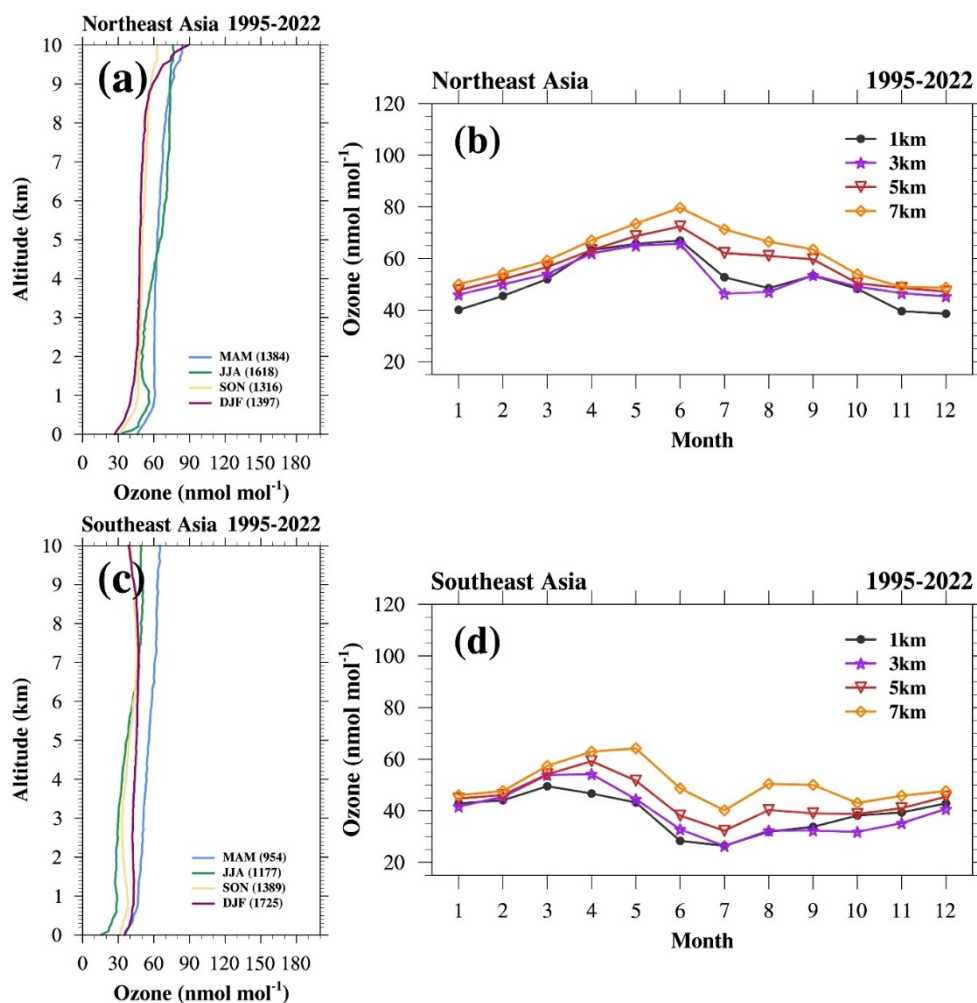


Figure 14. Analysis of the IAGOS measurements: (a) seasonal mean vertical ozone profiles in Northeast Asia during March-April-May (MAM, blue), June-July-August (JJA, green), September-October-November (SON, orange), and December-January-February (DJF, red), (b) monthly mean ozone variation of 1-km (black), 3-km (purple), 5-km (red), and 7-km (orange) altitudes in Northeast Asia. (c) same seasonal mean vertical ozone profiles but in Southeast Asia, and (d) same monthly mean ozone variation but in Southeast Asia. The number in the parenthesis in panel (a) and (c) indicates the number of used data for each season.

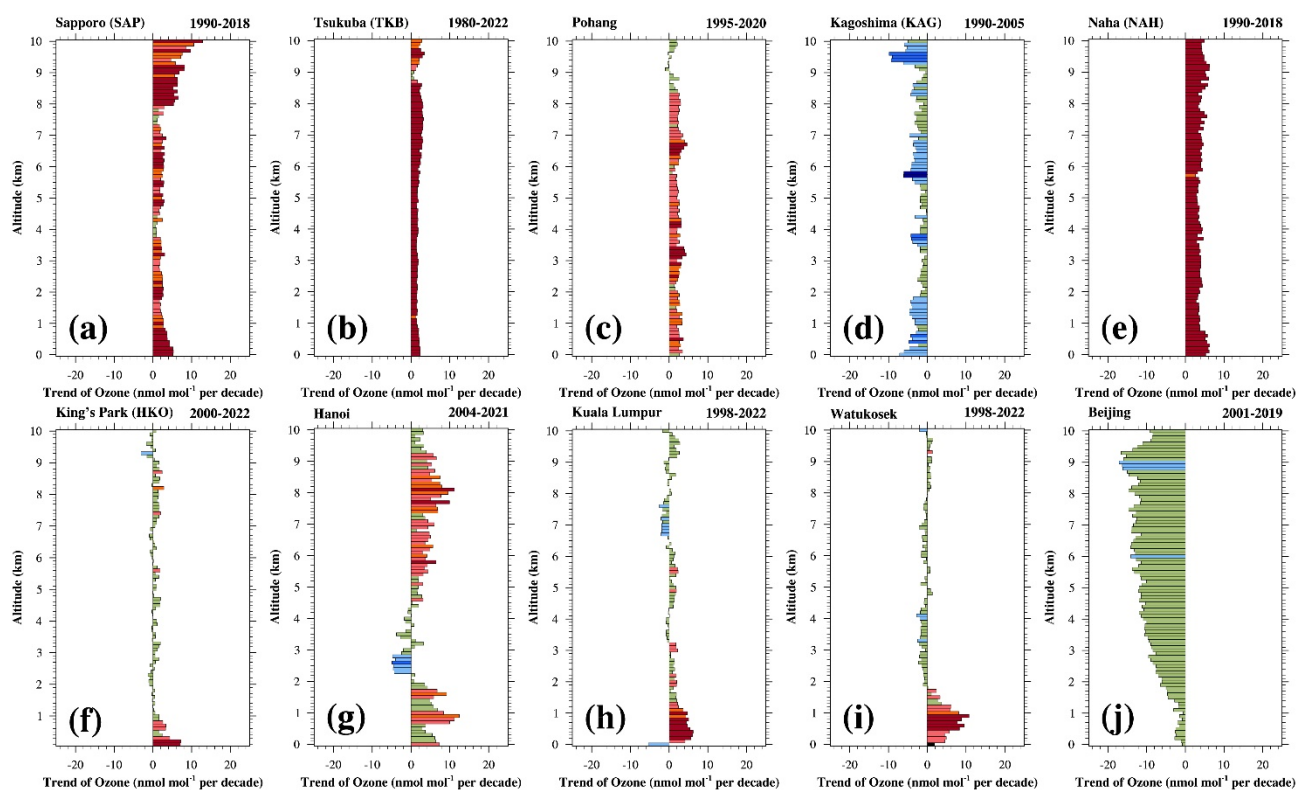


Figure 15. Long-term trends of annual median ozone per 100-m range from 0 to 10 km altitude at (a) Sapporo, (b) Tsukuba, (c) Pohang, (d) Kagoshima, (e) Naha, (f) King's park, (g) Hanoi, (h) Kuala Lumpur, (i) Watukosek, and (j) Beijing site. Dark red color means positive trend values with $p \leq 0.05$ (high certainty), orange color means positive trend values with $0.05 < p \leq 0.10$ (medium certainty), light orange color means positive trend values with $0.10 < p \leq 0.33$ (low certainty), light olive green color means positive/negative trend values with $p > 0.33$ (no evidence), light blue means negative trend values with $0.10 < p \leq 0.33$ (low certainty), medium blue color means negative trend values with $0.05 < p \leq 0.10$ (medium certainty), and dark blue color means negative trend values with $p \leq 0.05$ (high certainty).

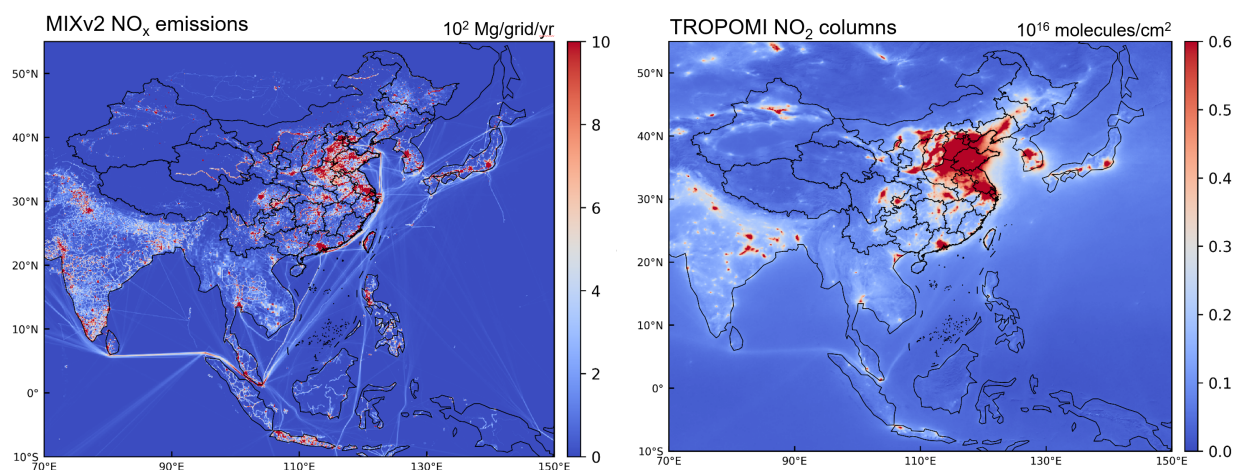


Figure 16. The spatial distribution of bottom-up NO_x emissions from MIXv2 inventory (left) and the TROPOMI satellite derived NO_2 columns (right). Due to the data availability, emission data for year 2017 and satellite data for year 2019 are used to represent the present-day level (2017-2021), respectively.